General Disclaimer

One or more of the Following Statements may affect this Document

- This document has been reproduced from the best copy furnished by the organizational source. It is being released in the interest of making available as much information as possible.

- This document may contain data, which exceeds the sheet parameters. It was furnished in this condition by the organizational source and is the best copy available.

- This document may contain tone-on-tone or color graphs, charts and/or pictures, which have been reproduced in black and white.

- This document is paginated as submitted by the original source.

- Portions of this document are not fully legible due to the historical nature of some of the material. However, it is the best reproduction available from the original submission.

N.A.S.A. NGR-47-018-005

VMI RESEARCH LABORATORIES

VIRGINIA MILITARY INSTITUTE
LEXINGTON, VIRGINIA
24450

DIGITAL ADAPTIVE CONTROL OF A VTOL AIRCRAFT

FINAL REPORT

NOVEMBER 1973 - AUGUST 1976

CONTRACT: NGR 47-018-005

PRINCIPAL INVESTIGATOR: Dr. Gerald F. Reid

INSTITUTION: Virginia Military Institute

Lexington, Virginia 24450

TABLE OF CONTENTS

ABSTRACT

A technique has been developed for calculating feed-back and feed-forward gain matrices that stabilize a VTOL aircraft while enabling it to track input commands of forward and vertical velocity. Leverrier's algorithm is used in a procedure for determining a set of state-variable, feedback gains that force the closed-loop poles and zeroes of one pilot-input transfer function to be at pre-selected positions in the s-plane. This set of feedback gains is then used to calculate the feedback and feedforward gains for the velocity-command controller. The method is computationally attractive since the gains are determined by solving systems of linear, simultaneous equations. Responses obtained using a digital simulation of the longitudinal dynamics of the CH-47 helicopter are presented.

LIST OF FIGURES

1. INTRODUCTION

1.1 Background

In recent years the overcrowding of this country's major airports has
led to increased interest in the development of commerical VTOL or STOL air-
craft capable of operating in the 0-500 mile range. These vehicles would
operate from separate runways at existing airports or from rooftops or short
runways in or near business districts. Studies have shown (1,2) that such
aircraft could reduce the total trip time providing they don't have to
operate under existing take-off and landing procedures with their long
delays. This will require innovations in vehicle design plus improved
navigation, guidance, and control systems. One approach to this latter
problem is to use on-board digital computers to handle the navigation,
guidance, and control functions in an adaptive mode. Thus it is necessary
to have a controller capable of following guidance commands from the computer
and at the same time present acceptable flying qualities to pilot inputs.

The Flight Instrumentation Division of NASA's Langley Research Center
is developing a technology base for digital adaptive control systems under
the VTOL Advanced Landing Technology (VALT) program. This work was supported
under this program by grant number NGR 47-018-005.

1.2 Summary of Results

This report presents the results of an investigation to develop a control
algorithm as described above. The approach used in this investigation was to
employ state variable feedback to achieve pole-zero placement of the vehicle's
transfer functions. The initial attempt was to use the modified Newton-
Ralphson technique to determine the necessary gains. This presented several
difficulties, which are discussed later, and was abandoned in favor of a

procedure, based on Leverrier's algorithm, that only requires the solution of linear simultaneous equations.

Using this procedure one first calculates a set of state-variable feedback gains that result in acceptable responses to pilot inputs. This set of gains is then used to generate two sets of gains, one feedback and one feedforward, that maintain the same response to pilot inputs but enable the vehicle to track velocity commands from the guidance system. The algorithm is then used to control longitudinal dynamics in a digital simulation of the CH-47 helicopter during a decelerating approach. With this functioning properly, studies are conducted to demonstrate the controller's ability to function in the presence of errors in the estimates of aircraft parameters and at different sampling rates.

1.3 Report Outline

The equations and algorithms needed to express the coefficients of the closed-loop transfer function numerator and denominator polynomials are developed in Section 2. In Section 3 the various methods used to calculate the feedback gains are discussed along with some considerations in selecting a model. Section 4 presents the velocity-command configuration and procedure for calculating the necessary gains. In Section 5 the results of several fixed-point simulations are presented along with the simulation of a decelerating approach. Section 6 contains the results of the studies on varying aircraft parameters and sampling time.

2. ANALYTICAL DEVELOPMENT

2.1 Basic Concepts

In considering the longitudinal dynamics of the CH-47 helicopter, the linearized equations of motion may be written in the form

$$\dot{\underline{x}} = A\underline{x} + G\underline{\delta} \tag{2-1}$$

where

$$\underline{x} = \begin{bmatrix} u \text{ (forward velocity perturbation)} \\ w \text{ (vertical velocity perturbation)} \\ q \text{ (pitch rate)} \\ \theta \text{ (pitch angle perturbation)} \end{bmatrix}$$

$$\underline{\delta} = \begin{bmatrix} \delta_e \text{ (differential collective purturbation)} \\ \delta_c \text{ (collective perturbation)} \end{bmatrix}$$

A is the 4 x 4 differential transition matrix

G is the 4 x 2 input matrix

Introducing state-variable feedback from all states to both inputs results in a control vector of the form

$$\underline{\delta} = K\underline{x} + \underline{\delta}_p \tag{2-2}$$

where

K is a 2 x 4 matrix of feedback gains

$\underline{\delta}_p$ is a 2 vector of pilot commands

Applying this control to equation (2-1) yields

$$\dot{\underline{x}} = (A + GK)\underline{x} + G\underline{\delta}_p \tag{2-3}$$

The Laplace transform of equation (2-3) is

$$[sI - (A + GK)]\underline{x}(s) = G\underline{\delta}_p(s) \tag{2-4}$$

This equation leads to eight closed-loop transfer functions relating the four state variables to the two controls. These transfer functions may be obtained by employing Cramer's rule. Thus, they all have the same denominator, $|sI - (A + GK)|$, but different numerators that are obtained by taking the determinants of the matrices that result when the appropriate columns of the G matrix are substituted for columns of $[sI - (A + GK)]$. Each transfer function is a ratio of polynominals in s and the coefficients in these polynomials are functions of K. If values of K can be found to force these coefficients to take on pre-determined values, then the poles and zeroes of the closed-loop transfer functions can be placed anywhere in the s-plane.

The determination of these coefficients requires the expansion of 4 x 4 matrices where each element in the matrix is a function of the feedback gains. To do this by hand is an extremely tedious and error prone process. To avoid having to expand these determinants by hand, a procedure was developed, based on Leverrier's algorithm, that calculates the desired coefficients.

2.2 Leverrier's Algorithm

Leverrier's algorithm is presented, with a proof, in reference (3) and used by Montgomery and Hatch (4) in their differential synthesis approach to pole-zero placement. The algorithm is an efficient computational technique for generating the coefficients of a system's open-loop transfer functions, or of the closed-loop transfer functions provided the feedback gains are known.

In presenting the algorithm, consider equation (2-4) rewritten for an n x n open-loop system as

$$\underline{x}(s) = [sI - A]^{-1} G \underline{\delta}_p(s) \qquad (2-5)$$

The term $(sI - A)^{-1}$ is of primary importance and may be written in the form

$$(sI - A)^{-1} = \frac{B_1 s^{n-1} + B_2 s^{n-2} + \ldots + B_{n-1} s + B_n}{s^n + d_1 s^{n-1} + d_2 s^{n-2} + \ldots + d_{n-1} s + d_n} \quad (2\text{-}6)$$

where

B_i is an n x n matrix

d_i is a scalar coefficient of the characteristic equation.

These B matrices and d coefficients are generated by Leverrier's algorithm as presented below:

$$B_1 = I \qquad\qquad d_1 = - \text{trace } (B_1 A)$$

$$B_2 = B_1 A + d_1 I \qquad\qquad d_2 = - 1/2 \text{ trace } (B_2 A)$$

$$\vdots \qquad\qquad\qquad\qquad \vdots$$

$$\hspace{8cm} (2\text{-}7)$$

$$B_k = B_{k-1} A + d_{k-1} I \qquad\qquad d_k = - 1/k \text{ trace } (B_k A)$$

$$\vdots \qquad\qquad\qquad\qquad \vdots$$

$$B_n = B_{n-1} A + d_{n-1} I \qquad\qquad d_n = - 1/n \text{ trace } (B_n A)$$

The transfer function between the ith state and j^{th} input is of the form

$$\frac{x_i}{\delta_j} = \frac{\alpha_{ij1} s^{n-1} + \alpha_{ij2} s^{n-2} + \ldots + \alpha_{ijn}}{s^n + d_1 s^{n-1} + d_2 s^{n-2} + \ldots d_{n-1} s + d_n} \quad (2\text{-}8)$$

where the denominator is the same as in equation (2-6) and the α's can be computed from

$$\alpha_{ijk} = \underline{u}_i^T B_k G \underline{u}_j \quad (2\text{-}9)$$

The $\underline{u}_i$ and $\underline{u}_j$ are commensurable unit vectors with 1 in the ith and j^{th} positions respectively and 0 elsewhere.

Thus the open-loop transfer function coefficients can be calculated, but

what is needed are the closed-loop coefficients expressed as functions of the feedback gains.

2.3 Expansion of the Closed-Loop Denominator

To achieve this consider the matrix $[sI - (A + GK)]$ rewritten as

$$[(s\underline{u}_1 - \underline{a}_1 - \underline{g}_1 k_{11} - \underline{g}_2 k_{21})(s\underline{u}_2 - \underline{a}_2 - \underline{g}_1 k_{12} - \underline{g}_2 k_{22})$$
$$(s\underline{u}_3 - \underline{a}_3 - \underline{g}_1 k_{13} - \underline{g}_2 k_{23})(s\underline{u}_4 - \underline{a}_4 - \underline{g}_1 k_{14} - \underline{g}_2 k_{24})] \qquad (2\text{-}10)$$

where

$\underline{u}_i$ is a column vector with 1 in the ith position and 0 elsewhere

$\underline{g}_i$ is the ith column of the control matrix

$\underline{a}_i$ is the ith column of the open-loop A matrix

The determinant of this matrix is the closed-loop characteristic equation. Expanding this determinant using the rule

$$|\underline{a}_1 \ \underline{a}_2 \ (\underline{a}_3 + \underline{c}k_1) \ \underline{a}_4| = |\underline{a}_1 \ \underline{a}_2 \ \underline{a}_3 \ \underline{a}_4| + k_1 \ |\underline{a}_1 \ \underline{a}_2 \ \underline{c} \ \underline{a}_4| \qquad (2\text{-}11)$$

results in

$$D_{CL} = D_{OL} - \sum_{i=1}^{2} \sum_{j=1}^{4} k_{ij} N(x_j, \delta_i) + \sum_{i=1}^{4} \sum_{\substack{j=1 \\ j \neq i}}^{4} k_{1i} k_{2j} N\left(\begin{smallmatrix} x_i, \delta_e \\ x_j, \delta_c \end{smallmatrix}\right) \qquad (2\text{-}12)$$

where

$$D_{OL} = |\underline{a}_1(s) \ \underline{a}_2(s) \ \underline{a}_3(s) \ \underline{a}_4(s)|$$

$$N(u, \delta_e) = |\underline{g}_1 \ \underline{a}_2(s) \ \underline{a}_3(s) \ \underline{a}_4(s)|$$

$$N\left(\begin{smallmatrix} u, \delta_e \\ q, \delta_c \end{smallmatrix}\right) = |\underline{g}_1 \ \underline{a}_2(s) \ \underline{g}_2 \ \underline{a}_3(s)|$$

D_{OL} is the open-loop denominator and $N(x_i, \delta_j)$ is the numerator of the x_i / δ_j open-loop transfer function. These terms are easily generated using equations (2-7) and (2-9). The $N\left(\begin{smallmatrix} x_i, \delta_e \\ x_j, \delta_c \end{smallmatrix}\right)$, which will be referred to as coupling functions, are not directly obtainable using Leverrier's algorithm.

2.4 Determination of the Coupling Functions

To develop the algorithm that generates $N\left(\begin{smallmatrix}x_i,\delta_e\\x_1,\delta_c\end{smallmatrix}\right)$, consider the matrix

formed by substituting the first column of the G matrix, times minus one, for

the first column of the A matrix

$$A' = [-\underline{g}_1 \ \underline{a}_2 \ \underline{a}_3 \ \underline{a}_4] \tag{2-13}$$

If Leverrier's algorithm is applied directly to the above A' matrix, one

obtains

$$[sI - A']^{-1} = \frac{B(s)}{d(s)} = \frac{B_1 s^3 + B_2 s^2 + B_3 s + B_4}{s^4 + d_1 s^3 + d_2 s^2 + d_3 s + d_4} \tag{2-14}$$

However, what is needed is an expression for

$$[sU_1 - A']^{-1} = \begin{bmatrix} g_{11} & -a_{21} & -a_{13} & -a_{14} \\ g_{21} & (s-a_{22}) & -a_{23} & -a_{24} \\ g_{31} & -a_{32} & (s-a_{33}) & -a_{34} \\ g_{41} & -a_{42} & -a_{43} & (s-a_{44}) \end{bmatrix}^{-1} \tag{2-15}$$

where

$$U_1 = \begin{bmatrix} 0 & 0 & 0 & 0 \\ 0 & 1 & 0 & 0 \\ 0 & 0 & 1 & 0 \\ 0 & 0 & 0 & 1 \end{bmatrix}$$

If B matrices and d coefficients, similar to those of equation (2-7), can

be found for this matrix, then the coefficients of the coupling terms can be

found by using equation (2-9) to solve a new system

$$[sU_i - A']\underline{y}(s) = \underline{g}_2 \tag{2-16}$$

where $\underline{y}(s)$ is an n-vector of polynomials and all but the ith element are

coupling functions.

7

Considering the form of equation (2-15), it is apparent that $[sU_1 - A']^{-1}$ can be written as

$$[sU_1 - A]^{-1} = \frac{B_1's^3 + B_2's^2 + B_3's + B_4'}{d_1's^3 + d_2's^2 + d_3's + d_4'} \tag{2-17}$$

where the denominator is $N(u, \delta_e)$, obtainable directly from Leverrier's algorithm.

Multiplying both sides of equation (2-17) by $[sU_1 - A']$ yields

$$[sU_1 - A'][B_1's^3 + B_2's^2 + B_3's + B_4'] =$$
$$[d_1's^3 + d_2's^2 + d_3's + d_4']I \tag{2-18}$$

Expanding this equation and equating like powers of s yields

$$U_1B_1' \qquad\qquad = 0$$
$$U_1B_2' - A'B_1' \quad = d_1'I$$
$$U_1B_3' - A'B_2' \quad = d_2'I \tag{2-19}$$
$$U_1B_4' - A'B_3' \quad = d_3'I$$
$$\qquad\quad - A'B_4' \quad = d_4'I$$

It was pointed out earlier that the d's are merely the coefficients of $N(u, \delta_e)$, which are known, and B_1' can be determined. However, knowing d_1' and B_1' does not allow one to solve for B_2' because U_1 is a singular matrix and therefore has no inverse.

Although the equations cannot be solved in the forward direction, they can be solved in reverse order if B_4' can be determined and if A' is not singular. In determining B_4' one must recall that it is the matrix of terms that do not contain s in the expression $[sU_1 - A']^{-1}$. Now recall that B_4 from equation (2-14) is the matrix of terms that do not contain s in the expression $[sI - A']^{-1}$. The only difference between $[sU_1 - A']$ and $[sI - A']$ is that

8

one of the diagonal elements of $[sI - A']$ is $(s + g_{ij})$ while for $[sU_1 - A']$ it is just g_{ij}. It is easy to show that the addition of s does not affect the B_4 matrix and therefore $B_4' = B_4$, a matrix generated by Leverrier's algorithm. Knowing B_4' equation (2-19) can be solved in reverse order

$$B_3' = A'^{-1}[U_1 B_4' - d_3' I]$$

$$B_2' = A'^{-1}[U_1 B_3' - d_2' I] \qquad (2\text{-}20)$$

$$B_1' = A'^{-1}[U_1 B_2' - d_1' I]$$

The procedure may be summarized as follows:

  1. Apply Leverrier's algorithm to the original A matrix and determine

$$D_{OL} = s^n + d_1 s^{n-1} + d_2 s^{n-2} + \dots + d_{n-1} s + d_n$$

$$N(u, \delta_e), \ N(w, \delta_e), \ N(q, \delta_e), \ N(\theta, \delta_e)$$

$$N(u, \delta_c), \ N(w, \delta_c), \ N(q, \delta_c), \ N(\theta, \delta_c)$$

  2. Replace one column of the A matrix with $-\underline{g}_1$ and apply Leverrier's algorithm to find B_4. Determine B's and $N\begin{pmatrix} u, \delta_e \\ w, \delta_c \end{pmatrix}$, $N\begin{pmatrix} u, \delta_e \\ q, \delta_c \end{pmatrix}$, $N\begin{pmatrix} u, \delta_e \\ \theta, \delta_c \end{pmatrix}$.

  3. Repeat step 2 for columns 2, 3, and 4 of the A matrix.

2.5 Closed-Loop Numerators

To determine the closed loop numerator coefficients as functions of the feedback gains, Cramer's rule can be used in conjunction with equation (2-11), to yield

$$N_{CL}(x_i, \delta_e) = N(x_i, \delta_e) - \sum_{\substack{j=1 \\ j \ne i}}^{4} k_{2j} N\begin{pmatrix} x_i, \delta_e \\ x_j, \delta_c \end{pmatrix} \qquad (2\text{-}21)$$

$$N_{CL}(x_i, \delta_c) = N(x_i, \delta_c) - \sum_{\substack{j=1 \\ j \ne i}}^{4} k_{1j} N\begin{pmatrix} x_i, \delta_c \\ x_j, \delta_e \end{pmatrix} \qquad (2\text{-}22)$$

Thus once the coupling function coefficients are known, both the closed-loop numerator and denominator polynomial coefficients may be determined as functions of K.

2.6 Chen's Algorithm

Since the development of the above algorithm for generating the coupling functions, the author has become aware of an algorithm developed by R.T.N. Chen (5) that will also generate these terms and which is more efficient computationally. The entire algorithm will not be developed here but the method of generating the coupling functions will be presented without proof. To simplify the expressions the following notation will be used:

$$
\underline{\psi}_1 \triangleq \begin{bmatrix} N(x_1, \delta_e) \\ N(x_2, \delta_e) \\ N(x_3, \delta_e) \\ N(x_4, \delta_e) \end{bmatrix} \qquad
\underline{\psi}_2 \triangleq \begin{bmatrix} N(x_1, \delta_c) \\ N(x_2, \delta_c) \\ N(x_3, \delta_c) \\ N(x_4, \delta_c) \end{bmatrix}
$$

Then the vectors of closed-loop numerators (using negative feedback) may be expressed as

$$
\underline{\psi}_{1_{CL}} = \underline{\psi}_1 + \frac{1}{D_{OL}} [\underline{\psi}_1 \underline{\psi}_2^T - \underline{\psi}_2 \underline{\psi}_1^T] \underline{k}_2 \tag{2-23}
$$

where $\underline{k}_2$ is the vector of δ_c feedback gains.

Comparing equations (2-23) and (2-22) it is apparent that the elements of the 4 x 4 matrix, $\frac{1}{D_{OL}} [\underline{\psi}_1 \psi_2^T - \psi_2 \psi_1^T]$, are the coupling functions. Since the diagonal elements of this matrix are zero there are three coupling functions per closed-loop numerator as previously determined. If one considers just one element of this matrix, for example the (1,2) element, it may be equated to a coupling function as shown below:

$$
N\left(\begin{matrix} x_1, \delta_e \\ x_2, \delta_c \end{matrix}\right) = \frac{N(x_1, \delta_e)N(x_2, \delta_c) - N(x_1, \delta_c)N(\delta_2, \delta_e)}{D_{OL}} \tag{2-24}
$$

The expression on the right hand side of the equal mark is the difference in two 6th order polynomials divided by a fourth order polynomial and it must yield a 2nd order polynomial with zero remainder because of the previous definition of the coupling functions.

Since all of the coefficients of the RHS polynomials of equation (2-24) are directly obtainable using Leverrier's algorithm, generating the coupling functions merely requires a subroutine to multiply and divide polynomials. Furthermore, since it is known that the remainder must be zero, it is not necessary to calculate all seven coefficients of the products $N(x_i, \delta_e)$ X $N(x_j, \delta_c)$ and only the first three in the division.

This approach has proven to be considerably more efficient than the previous method which involved four matrix inversions and many matrix multiplications.

3. DETERMINATION OF GAINS AND MODEL SELECTION

3.1 Determination of Feedback Gains

With the closed-loop transfer function coefficients expressed as functions of the feedback gains, the next step is to solve for a set of feedback gains that forces these coefficients to match predetermined values. This problem was approached from several different directions.

Initially only the poles of the system were placed by forming a weighted least squares cost function and using nonlinear minimization techniques to match the coefficients. While this does place the poles, it has the obvious disadvantage of offering no control over the zero locations. It also yields non-unique solutions since eight gains are available to match just four coefficients.

A second approach was to introduce a 2 x 2 cross-coupling matrix and then specify two numerator polynomials as well as the denominator. Again the gains were obtained by forming a weighted least squares cost function and minimizing using a modified Newton-Ralphson technique. This approach was never completely satisfactory because it invariably resulted in large values of gain or unacceptable responses for the transfer functions not being specified. This is most likely caused by the fact that u, w, and θ for the helicopter are not independent. If two of these values are specified then the third must take on whatever value is required to satisfy the other two. The problem then lies in the fact that it is very difficult to a priori specify two transfer functions that yield a satisfactory response for the third variable. The above methods are discussed in more detail in (6) and (7).

The method that was finally selected matches the poles and zeroes of one transfer function using only the feedback gains. Using this approach

it is only necessary to solve two systems of linear simultaneous equations. This method is presented by noting that the numerator coefficients are linear functions of elements of the gain matrix. If desired zero locations in the s-plane are specified, then a model numerator polynomial can be determined. Equating the coefficients of like powers of s in the model and equation (2-22) yields a system of three linear simultaneous equations that can be solved for three elements of the gain matrix. Depending on whether a δ_c or δ_e transfer function is selected, three of the four elements of the first or second row of the K matrix are uniquely defined. The fourth element may now be specified and these four known values of gain substituted into equation (2-12). When this is done, the denominator coefficients become linear functions of the remaining four elements of the gain matrix.

If the desired pole locations are now specified and a model characteristic equation formed, equating the coefficients of like powers of s results in a second linear system of simultaneous equations that may be solved for the remaining values of gain. The fact that the gains can be determined by solving two linear systems of simultaneous equations is a very attractive feature of this method and is discussed in more detail in reference (8).

3.2 Selection of a Model

While, in theory, the above technique is capable of generating feedback gains that can place the closed-loop poles and zeroes of one transfer function at arbitrary locations in the s-plane, in practice, considerable care must be exercised in specifying these values and in selecting the extra value of gain from the numerator equations. If these values are not carefully selected, either the gains will be too large or the other transfer functions of the system will have zero locations that result in unacceptable responses. Examples of this are presented in Section 5.

13

Initially the pole and zero locations were selected to match specifications set forth in references (9) and (10). This involved using pole-zero cancellation in order to match a second-order model and specifying two numerators. This effort was reported on in reference (11) but as stated previously, the general approach of trying to match two numerators did not produce satisfactory results and was abandoned.

The final method used was basically trial and error in an attempt to satisfy the specifications shown in figure (1). While no step-by-step procedure for selecting the pole-zero locations or the gain element can be given, the following general observations were made.

1. Moving the pole locations farther out into the left-hand-plane to improve the speed of response requires that the corresponding zero locations also be moved out if the steady-state response is to be maintained. This, in general, will increase the gain magnitudes.

2. In specifying the extra value of gain one should be aware of the relative magnitude of the state that the gain will multiply and the maximum allowable input to the system. This will allow an initial guess that is reasonable.

3. Once the open-loop numerator, denominator and coupling function coefficients have been determined, it is quite easy to iterate on the pole-zero locations and extra gain to determine a set of acceptable values.

4. For the CH-47, it required little modification to find acceptable values for all flight conditions considered, once an acceptable set of values were determined at one flight condition.

5. Right-half-plane zeroes, while not desirable, will not necessarily cause problems if they are far enough out in the RHP or if the magnitude of the transfer function's response is small.

14
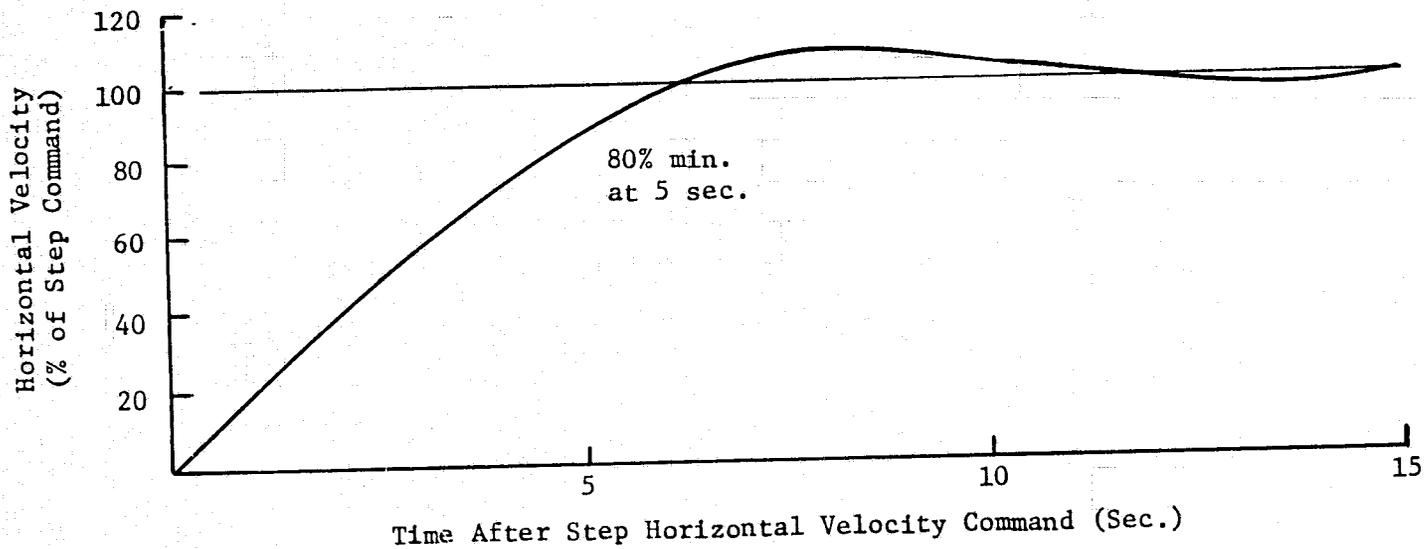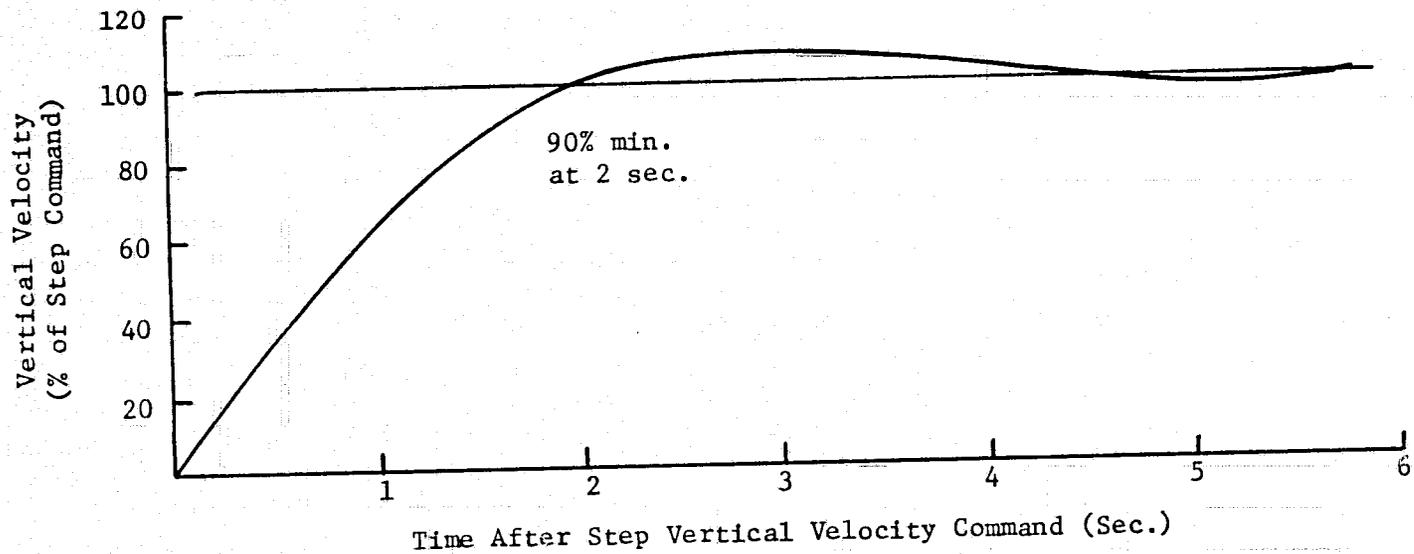
Figure (1) Typical Acceptable Responses To Velocity Commands

4. CLOSED-LOOP VELOCITY-COMMAND CONTROLLER

Once the elements of the gain matrix have been determined so that the step input responses of all transfer functions are acceptable, then a satisfactory pilot-command control system of the form shown in figure (2) has been generated.
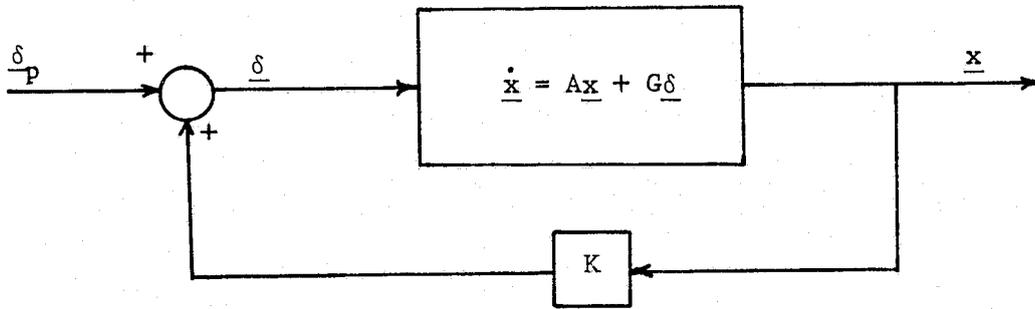

Figure (2) System Configuration for Pilot-Command Controller

With the above system it is possible, using the steady state responses of the transfer functions, to calculate the control inputs required to produce command changes in forward and vertical velocity (u_c and w_c). However, this would be an open-loop controller with the inherent disadvantages of open-loop systems. To overcome this, the system configuration of figure (3) was proposed.
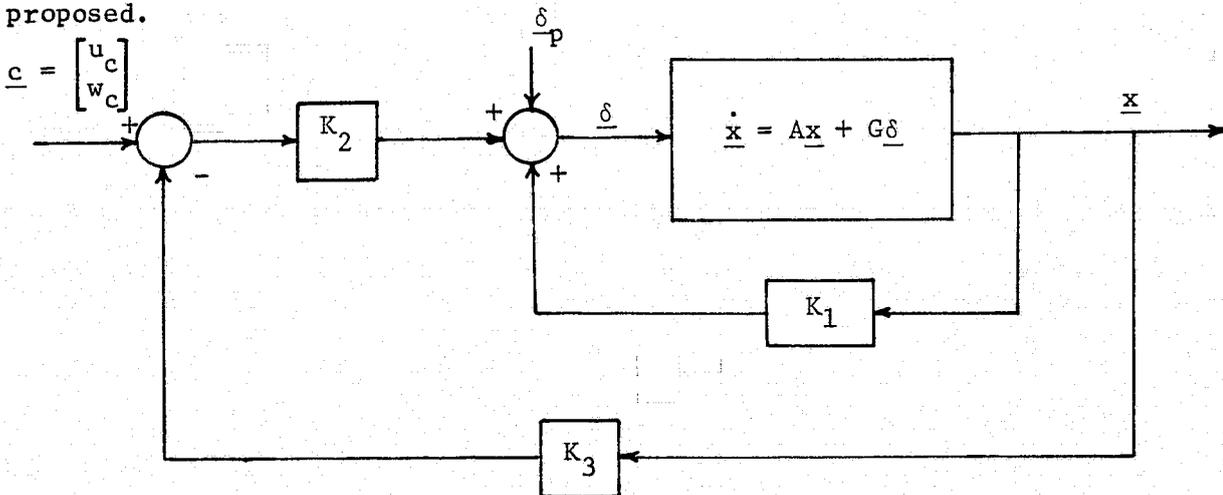
Figure (3) System Configuration for Velocity-Command Controller

where

$$K_3 = \begin{bmatrix} 1 & 0 & 0 & 0 \\ 0 & 1 & 0 & 0 \end{bmatrix}$$

K_2 is a 2 x 2 matrix of feedforward gains

K_1 is a 2 x 4 matrix of feedback gains

$\underline{c}$ is a 2 vector of command changes in u and w

The system dynamics are still defined by equation (2-1), but the input becomes

$$\underline{\delta} = K_1 \underline{x} + K_2 [\underline{c} - K_3 \underline{x}] \tag{4-1}$$

$$\underline{\delta} = K_1 \underline{x} - K_2 K_3 \underline{x} + K_2 \underline{c} \tag{4-2}$$

$$\underline{\delta} = [K_1 - K_2 K_3] \underline{x} + K_2 \underline{c} \tag{4-3}$$

or

$$\underline{\delta} = K \underline{x} + K_2 \underline{c} \tag{4-4}$$

Substituting into equation (2-1) yields

$$\dot{\underline{x}} = (A + GK) \underline{x} + GK_2 \underline{c} \tag{4-5}$$

Now let K be the set of feedback gains obtained by specifying the poles and zeroes of one of the pilot-command transfer functions. Then it is apparent that the velocity-command and pilot-command transfer functions will have the same poles. Employing Cramer's rule and equation (2-11) it can be shown that the numerators of the u/u_c, w/u_c, u/w_c, and w/w_c transfer functions may be expressed as

$$N(u,u_c) = k_{2_{11}} N_{c1}(u,\delta_e) + k_{2_{21}} N_{c1}(u,\delta_c) \tag{4-6}$$

$$N(w,u_c) = k_{2_{11}} N_{c1}(w,\delta_e) + k_{2_{21}} N_{c1}(w,\delta_c) \tag{4-7}$$

$$N(u,w_c) = k_{2_{12}} N_{c1}(u,\delta_e) + k_{2_{22}} N_{c1}(u,\delta_c) \tag{4-8}$$

$$N(w,w_c) = k_{2_{12}} N_{c1}(w,\delta_e) + k_{2_{22}} N_{c1}(w,\delta_c) \tag{4-9}$$

17

Each of the above equations represents a third order polynomial in s with four coefficients. While it is not possible to control all of the coefficients, it is possible to control one coefficient from each equation. If the system is to track velocity commands, the steady-state response of u and w to a unit step input on u_c must be one and zero respectively and the steady-state response of u and w to a unit step input on w_c must be zero and one respectively. This requires that the constant term of the numerator of the u/u_c transfer function equal the constant term of the denominator (which is known) and the constant term of the w/u_c transfer function equal zero to provide de-coupling. Placing these constraints on equations (4-6) and (4-7) yields two linear simultaneous equations to solve for $k_{2_{11}}$ and $k_{2_{21}}$. Similar restrictions on the constant terms of the w_c transfer functions result in two equations that yield $k_{2_{12}}$ and $k_{2_{22}}$. Once the values of K_2 are known K_1 can be determined using

$$K = [K_1 - K_2 K_3] \qquad (4\text{-}10)$$

18

5. SIMULATION RESULTS

This design procedure has been applied to the linearized longitudinal dynamics of the CH-47 helicopter. Results will be presented at several different flight conditions and finally the results of a simulated decelerating approach will be presented. The first example will be for nominal velocities of 150 kts. forward and 250 fpm vertical descent. This example will be used to demonstrate the technique for calculating K_2 in the velocity-command configuration.

5.1 Fixed Point I

The A and G matrices shown below are based on stability and control derivatives provided by NASA's Langley Research Center.

$$A = \begin{bmatrix} -0.05191 & -0.03898 & 8.8944 & -32.176 \\ 0.02731 & -0.57793 & 250.67 & 1.2324 \\ -0.00014 & 0.01769 & -1.3044 & 0 \\ 0 & 0 & 1.0 & 0 \end{bmatrix}$$

$$G = \begin{bmatrix} -0.14909 & -1.2698 \\ 0.01857 & -8.9842 \\ 0.31973 & 0.22782 \\ 0 & 0 \end{bmatrix}$$

The open-loop characteristic equation for this A matrix is

$$D_{OL} = s^4 + 1.934s^3 - 3.579s^2 - 0.221s + 0.0117$$

The sign changes in the coefficients indicate an unstable system and right-half-plane poles occur at 0.034 and 1.2.

Specifying the poles and zeroes of the w/δ_c transfer function as

19

Poles = -0.75, -0.8, -0.8 ± j0.4

Zeroes = -1.0, -0.8 ± j0.4

resulted in the following gain matrix:

$$K = \begin{bmatrix} 0.0667 & -0.02 & -23.75 & -5.17 \\ -0.0021 & 0.0034 & 28.08 & 0.324 \end{bmatrix}$$

when k_{12} was specified at -0.02. This feedback gain matrix yields denominator and numerator polynomials for pilot-command transfer functions as shown below with the steady-state response of each listed to the right.

	Steady-State Response/inch of control
$D_{CL} = s^4 + 3.15s^3 + 3.88s^2 + 2.2s + 0.48$	
$N(\delta_e, u) = 0.15s^3 - 9.23s^2 - 16.1s - 6.33$	-13.2 fps
$N(\delta_e, w) = 0.02s^3 - 0.6s^2 - s - 0.51$	-1.06 fps
$N(\delta_e, q) = 0.32s^3 + 0.21s^2 + 0.01s$	0
$N(\delta_e, \theta) = 0.32s^2 + 0.21s + 0.01$	0.02 rad
$N(\delta_c, u) = -1.27s^3 - 10.4s^2 - 11.4s - 1.58$	-3.29 fps
$N(\delta_c, w) = -8.98s^3 - 23.4s^2 - 21.6s - 7.19$	-15.0 fps
$N(\delta_c, q) = 0.228s^3 + 0.013s^2 - 0.006s$	0
$N(\delta_c, \theta) = 0.228s^2 + 0.013s - 0.006$	-0.013 rad

Thus, the system has been stabilized and the pilot-command responses, shown in figures (4) and (5), look reasonable. Sign changes in the u/δ_e, w/δ_e, and θ/δ_c numerators indicate right-half-plane zeroes; however, in u/δ_e and w/δ_e they are located at 64 and 34 respectively and do not seriously affect the responses. The θ/δ_c right-half-plane zero is at 0.14 and does cause some phase reversal. However, θ is not very responsive to δ_c commands and this may not be objectionable.

To determine the feedforward matrix, equations (4-6) - (4-9) are used

20
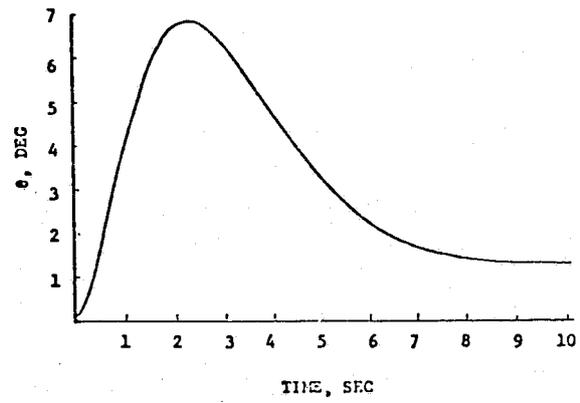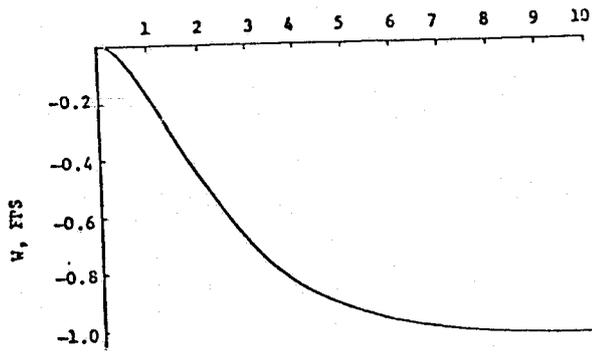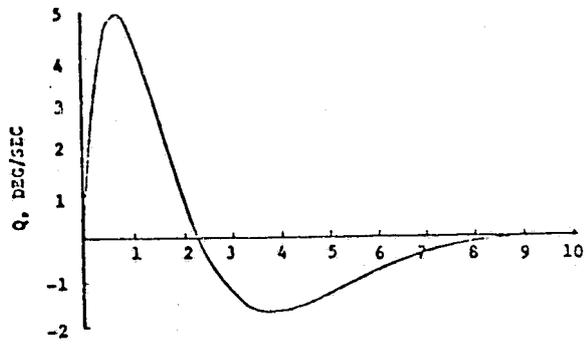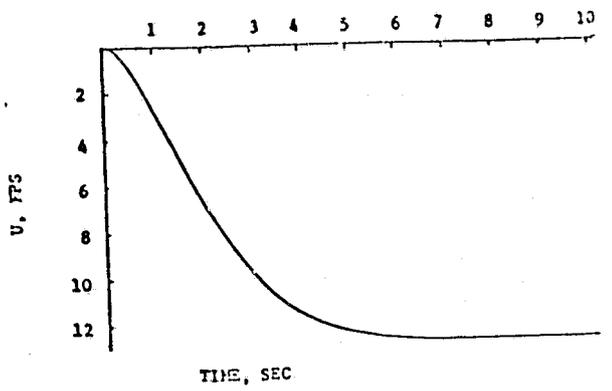
Figure (4) Responses to $\underline{\delta}_p^T = [1,0]$ for Fixed Point I
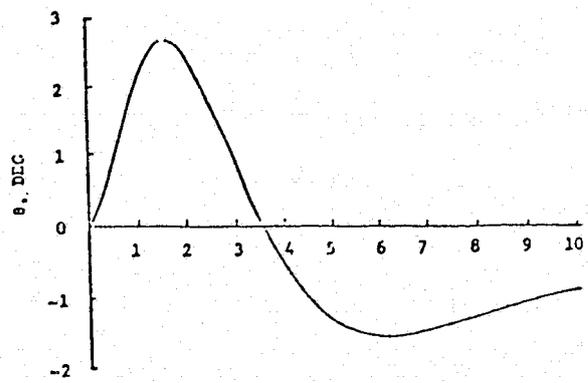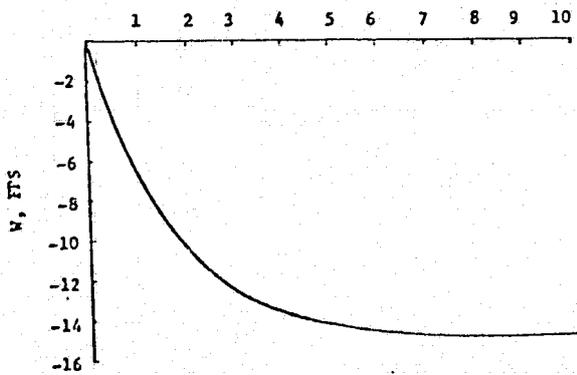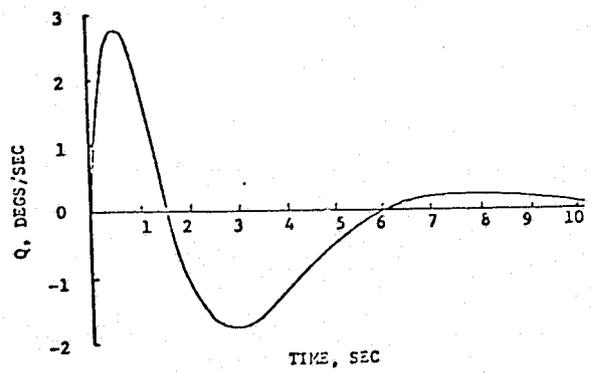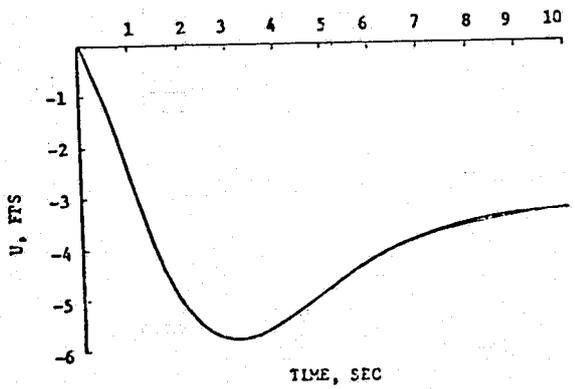
Figure (5) Responses to $\underline{\delta}_p^T = [0,1]$ for Fixed Point I

to form the following 2 x 2 systems of equations.

$$\begin{bmatrix} -6.33 & -1.58 \\ -0.51 & -7.19 \end{bmatrix} \begin{bmatrix} k_{2_{11}} \\ k_{2_{21}} \end{bmatrix} = \begin{bmatrix} 0.48 \\ 0 \end{bmatrix}$$

and

$$\begin{bmatrix} -6.33 & -1.58 \\ -0.51 & -7.19 \end{bmatrix} \begin{bmatrix} k_{2_{12}} \\ k_{2_{22}} \end{bmatrix} = \begin{bmatrix} 0 \\ 0.48 \end{bmatrix}$$

The resulting feedback and feedforward matrices are

$$K_1 = \begin{bmatrix} -0.0105 & -0.003 & -23.75 & -5.17 \\ 0.0034 & -0.065 & 28.08 & 0.324 \end{bmatrix}$$

$$K_2 = \begin{bmatrix} -0.0772 & 0.017 \\ 0.0054 & -0.068 \end{bmatrix}$$

These gains, used in the system configuration of figure (3), yield the following velocity-command transfer function numerators and steady-state responses:

		Steady-State Response to Unit Step Command
$N(u,u_c) = -0.018s^3 + 0.66s^2 + 1.17s + 0.48$		1.0
$N(w,u_c) = -0.050s^3 - 0.08s^2 - 0.04s + 0$		0.0
$N(q,u_c) = -0.023s^3 - 0.02s^2 - 0.0008s$		0.0
$N(\theta,u_c) = -0.023s^2 - 0.02s - 0.0008$		0.002 rad
$N(u,w_c) = 0.089s^3 + 0.553s^2 + 0.503s + 0$		0.0
$N(w,w_c) = 0.611s^3 + 1.58s^2 + 1.45s + 0.48$		1.0
$N(q,w_c) = -0.01s^3 + 0.003s^2 + 0.0006s$		0.0
$N(\theta,w_c) = -0.01s^2 + 0.003s + 0.0006$		0.001 rad

The responses to velocity commands of $\underline{c}^T = [10,0]$ and $\underline{c}^T = [0.10]$ were plotted and are shown in figures (6) and (7) respectively. The velocities settle to within 5% of the desired steady-state changes in 5 seconds with no overshoot and the decoupling between forward and vertical velocity commands is good. The pitch angle to vertical velocity command response shows a phase reversal that reaches a peak of 0.9 degrees in 1.3 seconds, but this may not be objectionable. If these responses were unacceptable to either pilots or passengers, the gains could easily be recalculated using new pole-zero specifications.

5.2 Fixed Point II

The results of the previous example do not completely satisfy the specifications of figure (1) in that the vertical velocity rise time exceeds two seconds. To correct this, the poles and zeroes of the w/δ_c transfer function were moved to the following locations

Poles = $-0.9 \pm j0.1$, $-0.9 \pm j0.45$

Zeroes = -1.0, $-0.9 \pm j0.1$

and k_{12} was specified at -0.03. The nominal velocities were set at 110 fps forward and 500 fpm vertical descent since these values correspond to desired values along one section of the nominal approach path shown in figure (8). The A and G matrices will not be listed for the remaining examples, but can be determined based on the data in reference (12). The K and K_2 matrices for this example are shown below

$$K = \begin{bmatrix} 0.075 & -0.030 & -7.126 & -5.765 \\ -0.046 & 0.050 & 12.412 & 2.156 \end{bmatrix}$$

$$K_2 = \begin{bmatrix} -0.062 & 0.039 \\ 0.007 & -0.108 \end{bmatrix}$$

23
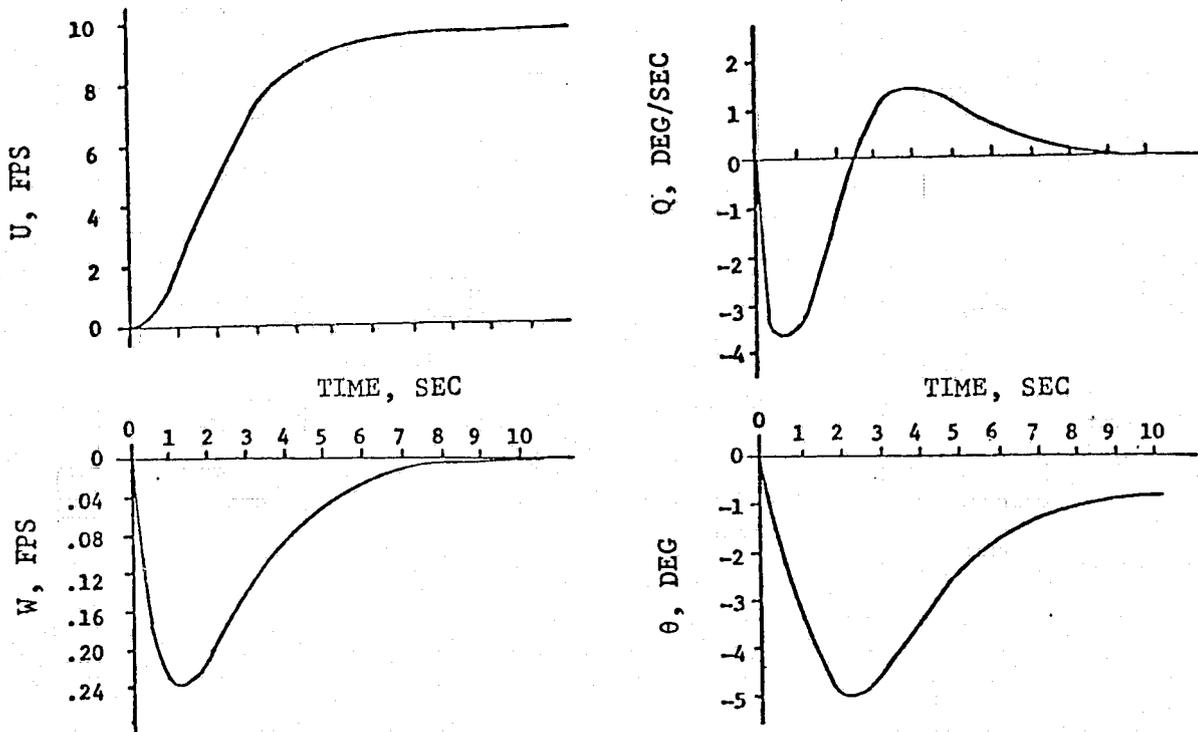
Figure (6) Responses to $\underline{c}^T = [10,0]$ for Fixed Point I
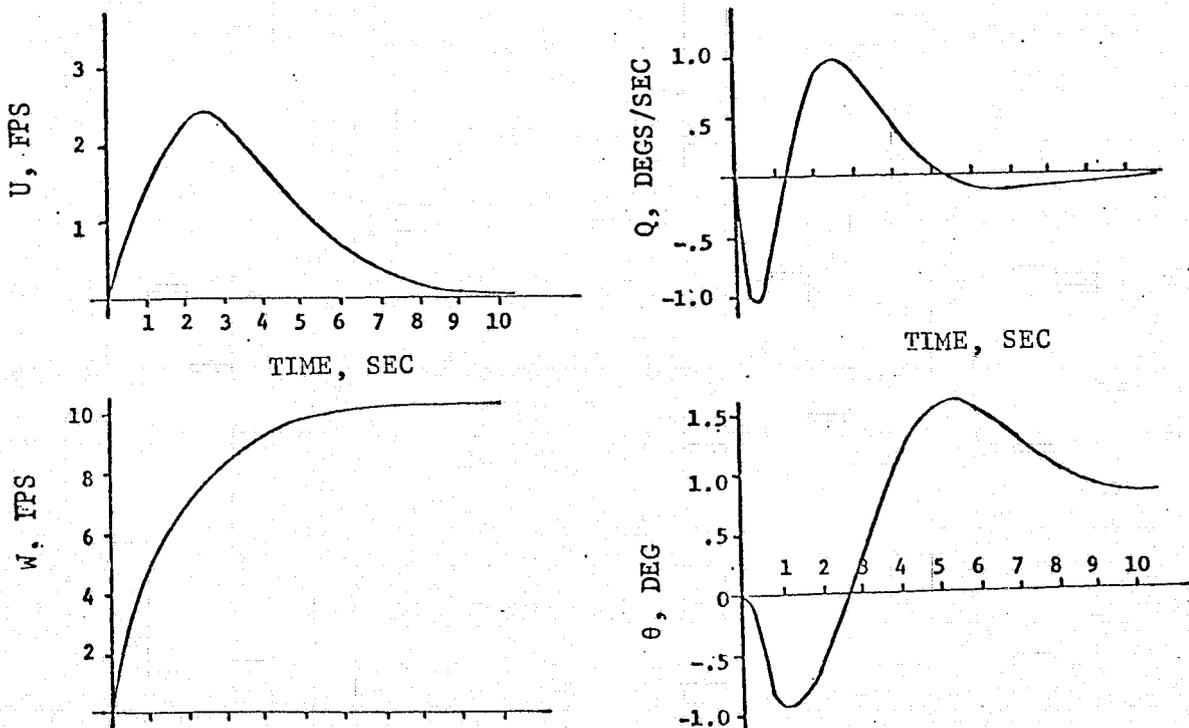
Figure (7) Responses to $\underline{c}^T = [0,10]$ for Fixed Point I

From B to C
w = 500 fpm
u = 110 fps

From A to B
z = 750 ft
w = 0 fps
u = 110 fps

From C to D
w = 500 fpm
u = see below
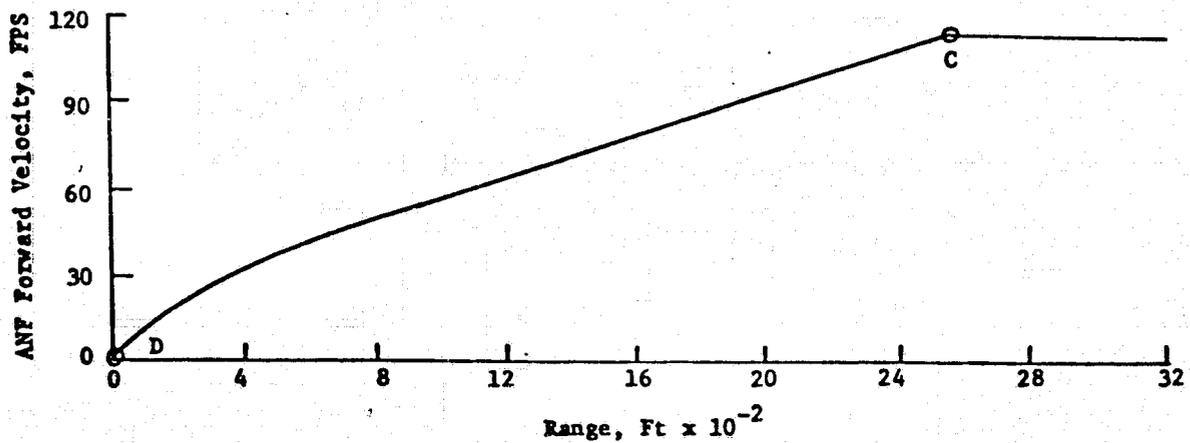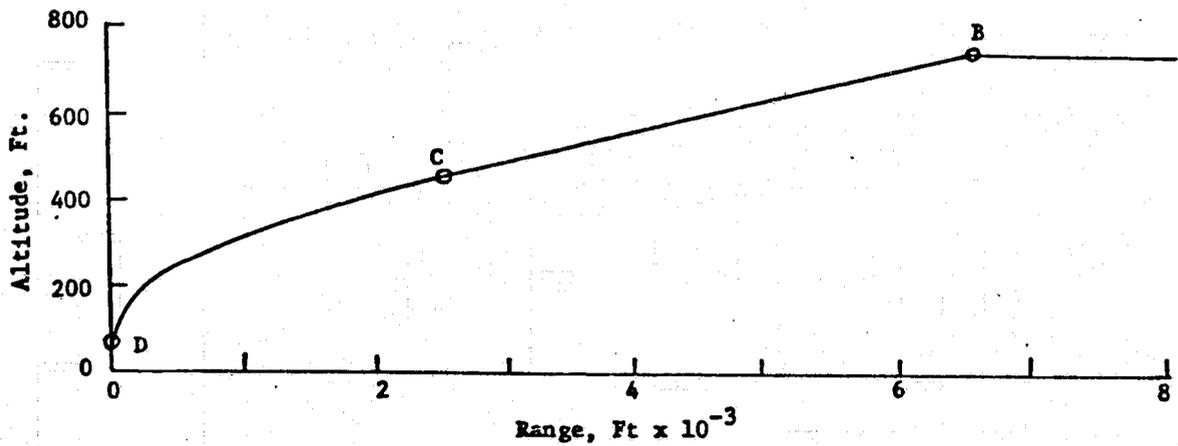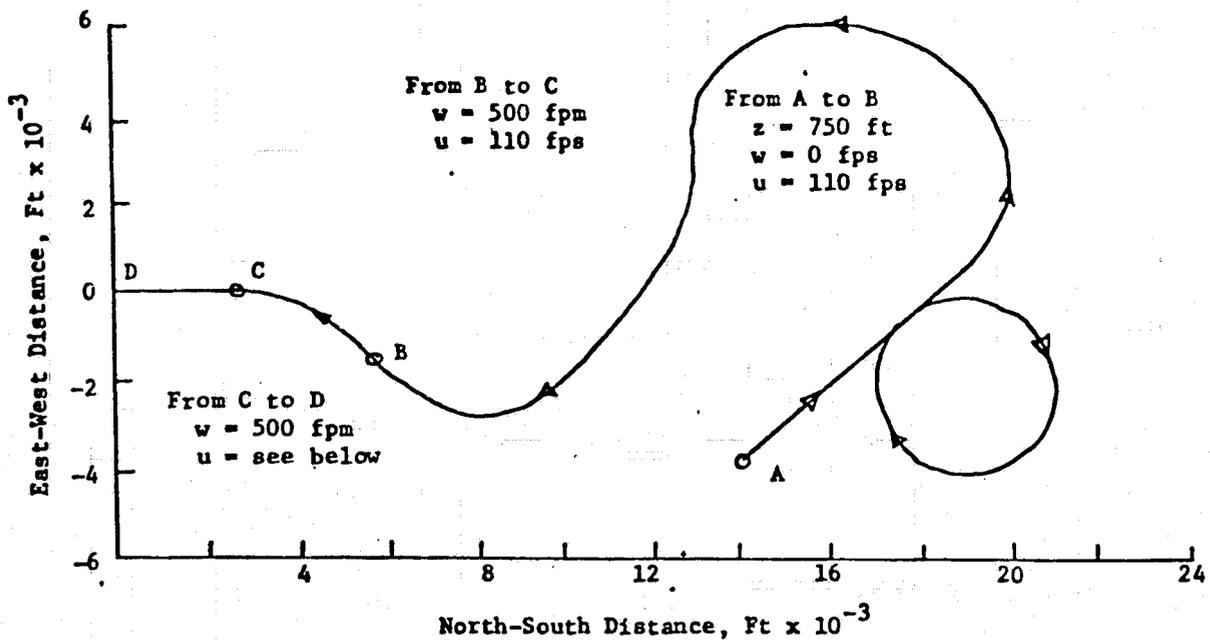
Figure (8) Nominal Approach Path

25

The corresponding plots of the velocity responses to pilot commands and velocity commands are shown in figures (9) and (10) respectively. These responses do satisfy the previously stated specifications and the decoupling between u and w in the velocity-command mode looks good. There is some direction reversal in the u/w_c response but because of the small peak value of this response it should not be objectionable. The pitch and pitch rate responses are not shown since they were acceptable and are not of primary concern in this study.

5.3 Fixed Point III

This example is included to emphasize the importance of achieving satisfactory responses to pilot inputs prior to determining the gains for the velocity-command loop. Before attempting to simulate a decelerating approach, the controller's ability to function properly at various nominal points throughout the flight range was investigated. In this example the nominal velocities were 20 fps forward and 3.33 fps vertical descent. The model and k_{12} were the same as in Example II. The velocity responses are shown in figures (11) and (12). The responses to δ_e commands show extreme coupling between u and w and a rather severe direction reversal on u/δ_c (again because of the small peak value this may not present a problem). The corresponding velocity-command responses demonstrate the same undesirable level of coupling between u and w for u_c commands. The peak value of 10 fps will most likely cause problems when flown in an adaptive mode. To correct this the value of k_{12} was adjusted (since it had been noted in previous studies that this can have considerable influence on the coupling between u and w) from -0.03 to +0.01. This yielded the responses shown in figures (13) and (14). The coupling has been greatly reduced and although the u/w_c response indicates a RHP zero the peak value is again small.
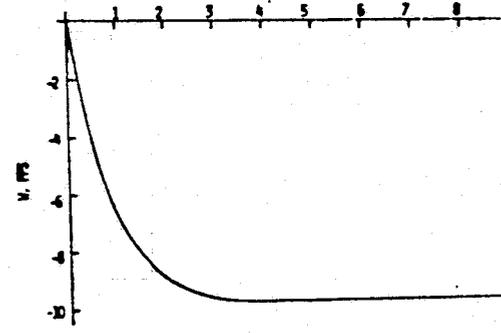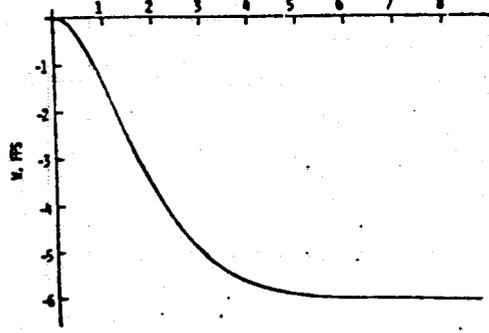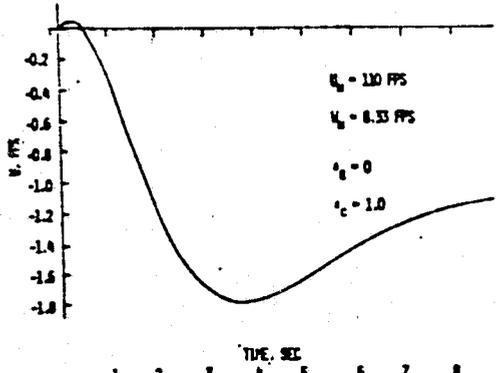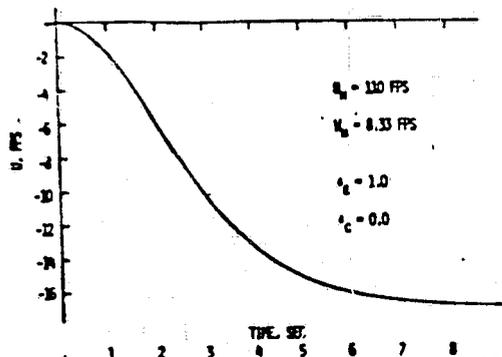
**Figure (9) Velocity Responses to Pilot Commands for Fixed Point II**
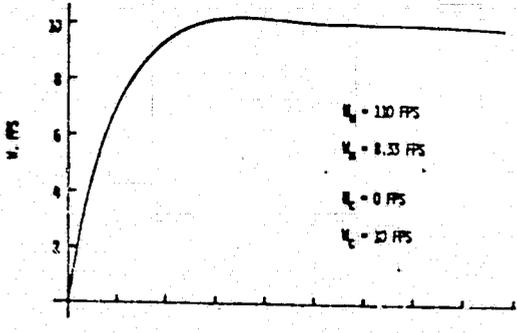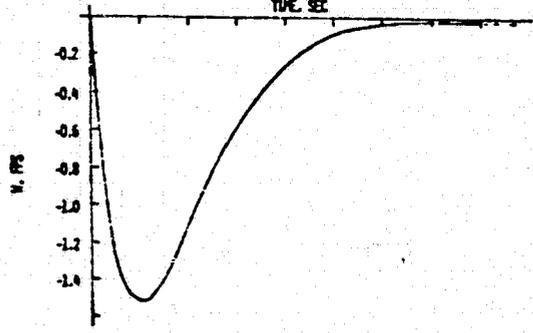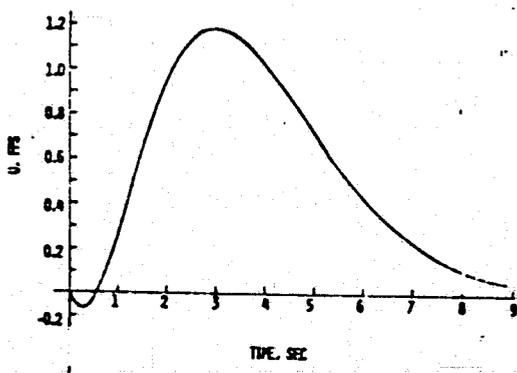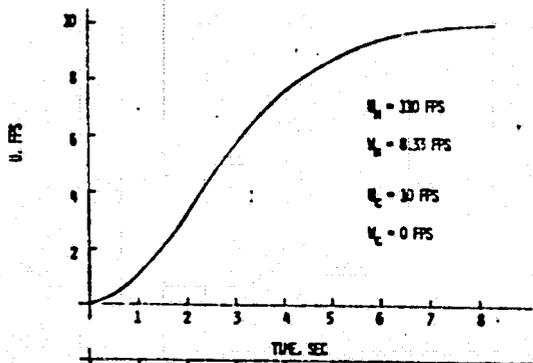
**Figure (10) Velocity Responses to Velocity Commands for Fixed Point II**
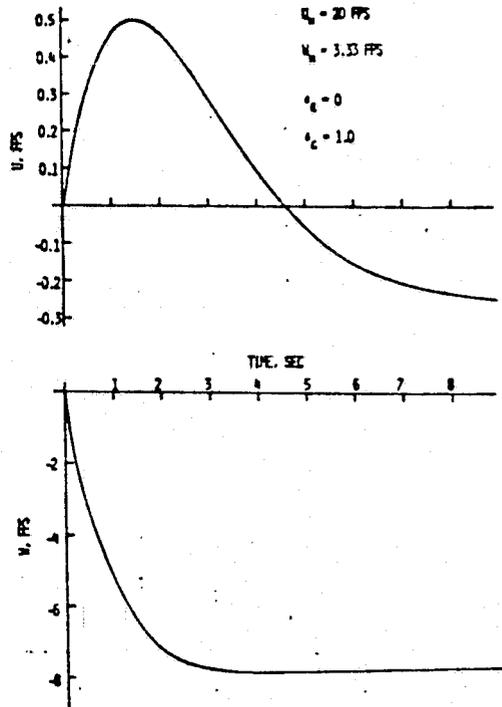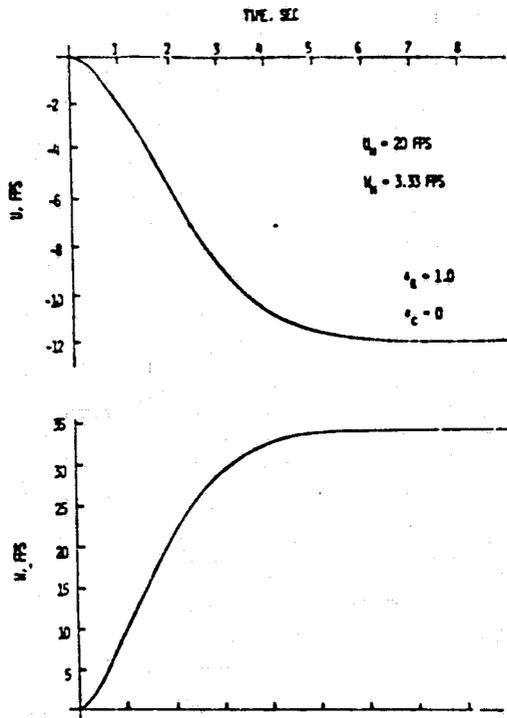
Figure (11) Velocity Responses to Pilot Commands for Fixed Point III (k_{12} = -0.03)
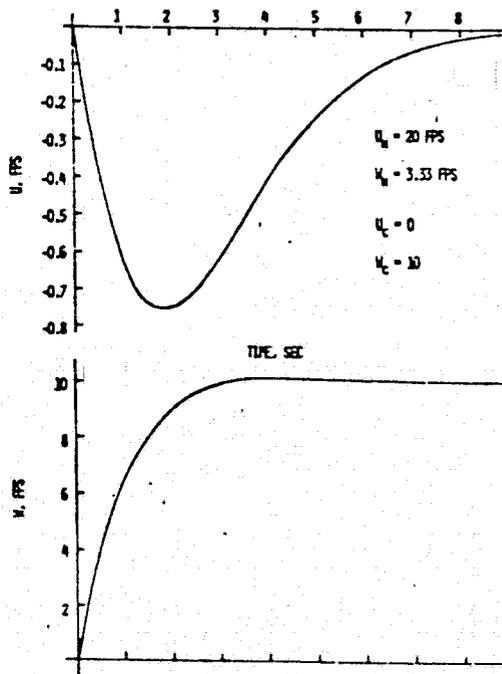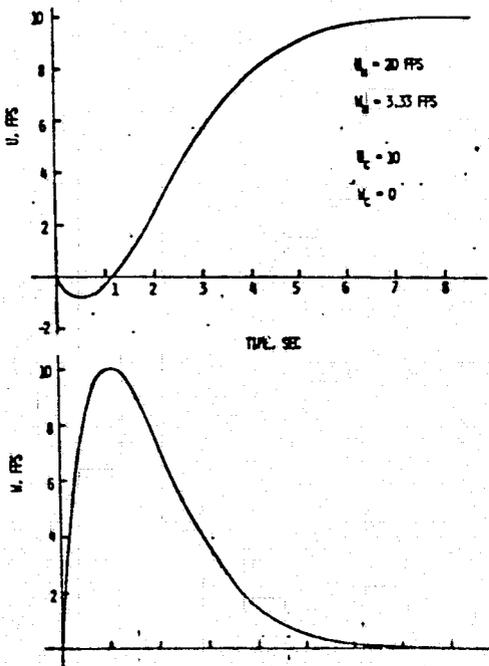
Figure (12) Velocity Reponses to Velocity Commands for Fixed Point III (k_{12} = -0.03)
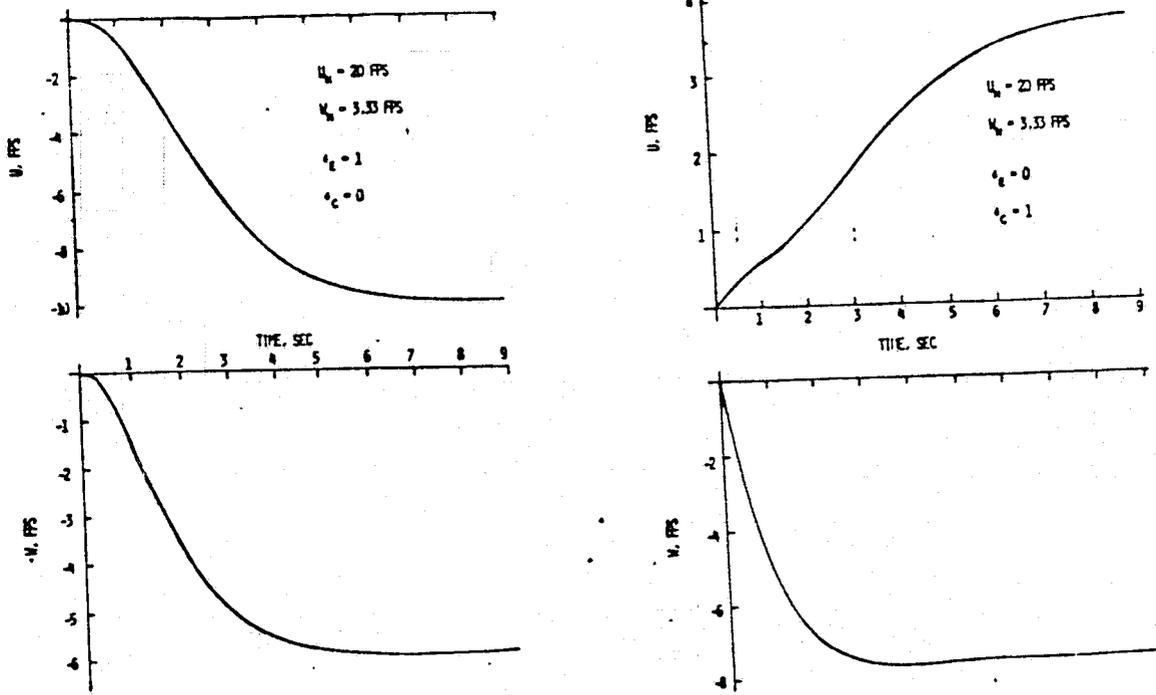
Figure (13) Velocity Responses to Pilot Commands for Fixed Point III ($k_{12} = 0.02$)
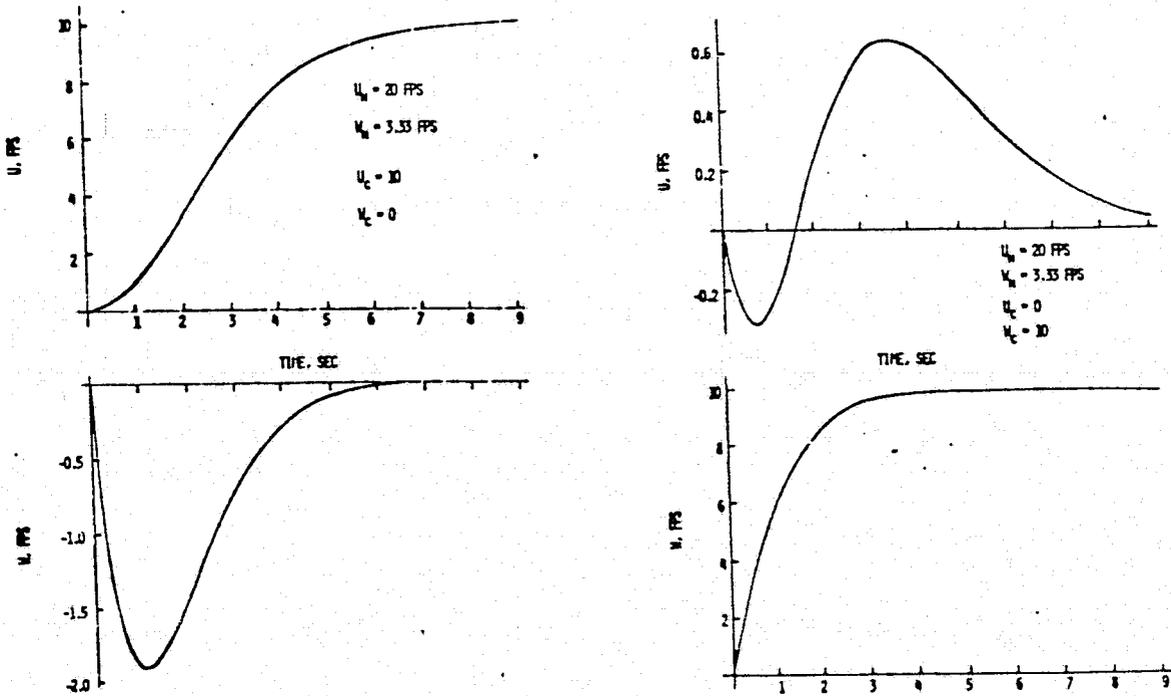
Figure (14) Velocity Responses to Velocity Commands for Fixed Point III ($k_{12} = 0.01$)

Using the model from Example II and $k_{12} = 0.01$ satisfactory responses were obtained at all flight conditions and these values were therefore used in the simulation of a decelerating approach.

5.4 Decelerating Approach

With the algorithm generating acceptable responses throughout the desired range of flight conditions, the next step was to check the controller's ability to function in an adaptive mode during a decelerating approach.

The section from C to D of the nominal approach path of figure (8) was used for this study with the following modifications.

1. The vertical velocity between B and C was set at 0 rather than 500 fpm. (The controller was checked under both conditions but the results presented are for the latter since this is a more severe test of its ability to come onto and remain on the desired path.)

2. The vertical velocity was linearly decreased from 500 fpm to 0 over the range from 100 feet to 0. This takes both forward and vertical velocities to zero simultaneously and brings the vehicle to hover at an altitude of 50 feet.

In order to simulate a decelerating approach a guidance law had to be developed that would command the changes in forward and vertical velocities necessary to keep the vehicle on the desired approach path. This requirement is complicated by the fact that the controller is designed to command changes in body axis velocities while the approach path is defined in terms of approach navigation frame (ANF) velocities. The relationship between these two axis systems is shown in figure (15).
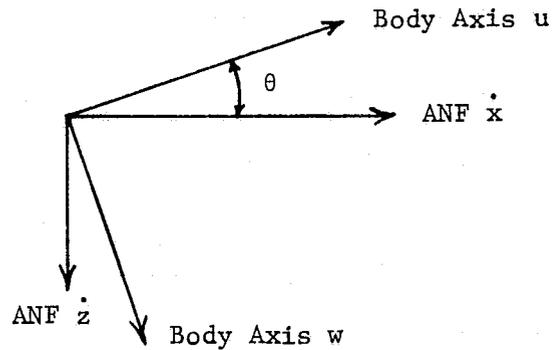
Figure (15) Relationship Between Body Axis and ANF Axis

These systems are related by the equations

$$u = \dot{x} \cos \theta - \dot{z} \sin \theta$$

$$w = \dot{x} \sin \theta + \dot{z} \cos \theta$$

(5-1)

Thus the basic procedure is to determine the desired changes in $\dot{x}$ and $\dot{z}$ and then use equation (5.1) to generate the necessary commands in u and w. The equations for generating $\dot{x}$ and $\dot{z}$ are of the form proposed by Hoffman, Zvara, Bryson, and Ham (13). The general procedure is to develop expressions for $\dot{x}$, $\dot{z}$, and z as functions of range and determine the necessary purturbations with the following equations:

$$\Delta\dot{x} = (\dot{x}_{DESIRED} - \dot{x}_{ACTUAL}) - c_x(z_{ACTUAL} - z_{DESIRED})$$

$$\Delta\dot{z} = (\dot{z}_{DESIRED} - \dot{z}_{ACTUAL}) + c_z(z_{ACTUAL} - z_{DESIRED})$$

(5-2)

where c_x and c_z are weighting factors whose function is to maintain the desired altitude profile. For the results to be presented $c_x = 0.5$ and $c_z = 1.5$. The equations expressing $\dot{x}$, $\dot{z}$, and z as functions of range are given below and were obtained by fitting curves to desired profiles of figure (8).

For $2500 \leq R < 1200$

$$\dot{x}_{DESIRED} = 0.0333 \cdot R + 26.0$$

$$\dot{z}_{DESIRED} = 8.333$$

(5-3)

$$z_{DESIRED} = -1.21212 \cdot R^2 + 0.1448484 \cdot R + 173.636$$

31

For $1200 \leq R < 400$

$$\dot{x}_{DESIRED} = -6.25 \cdot 10^{-6} \cdot R^2 + 0.0525 \cdot R + 12.0$$

$$\dot{z}_{DESIRED} = 8.333$$

$$z_{DESIRED} = -6.25 \cdot 10^{-5} \cdot R^2 + 0.275 \cdot R + 90.0$$

For $400 \leq R < 0$

$$\dot{x}_{DESIRED} = -1.0 \cdot 10^{-4} \cdot R^2 + 0.12 \cdot R$$

$$\dot{z}_{DESIRED} = \begin{cases} 8.3333 & 400 \leq R \leq 100 \\ 0.08333 & 100 < R \leq 0 \end{cases}$$

$$z_{DESIRED} = -5.0 \cdot 10^{-4} \cdot R^2 + 0.55 \cdot R + 50.0$$

In the $z_{DESIRED}$ equations the value of R is the actual value at the time the velocity commands are updated. For $\dot{x}_{DESIRED}$ and $\dot{z}_{DESIRED}$ the value of R is obtained by subtracting DT $\cdot \dot{x}_{ACTUAL}$, where DT is the guidance update time, from the actual value of R. This does not give an exact value for R and therefore $\dot{x}$ and $\dot{z}$ at the next update point since $\dot{x}$ is changing but it does yield an estimate at some future point along the trajectory and it was reasoned that this is better than commanding $\dot{x}$ and $\dot{z}$ based on the current location.

For the results to be presented the sampling rate was 10 per sec. and the guidance commands were updated every 0.5 sec. while the actual aircraft parameters and gains were updated every second. The model and value of k_{12} were the same as the last example at fixed point III.

The results of this simulation appear in figures (16) through (20). The plot of altitude vs. range shows good tracking while the ANF $\dot{x}$ vs. range curve shows the actual velocity consistantly above the desired value. It should be emphasized, however, that the guidance law, equation (5.2) penalizes errors in altitude so this result might have been anticipated. It should also be emphasized that this guidance law was rather hastily devised to test the

32
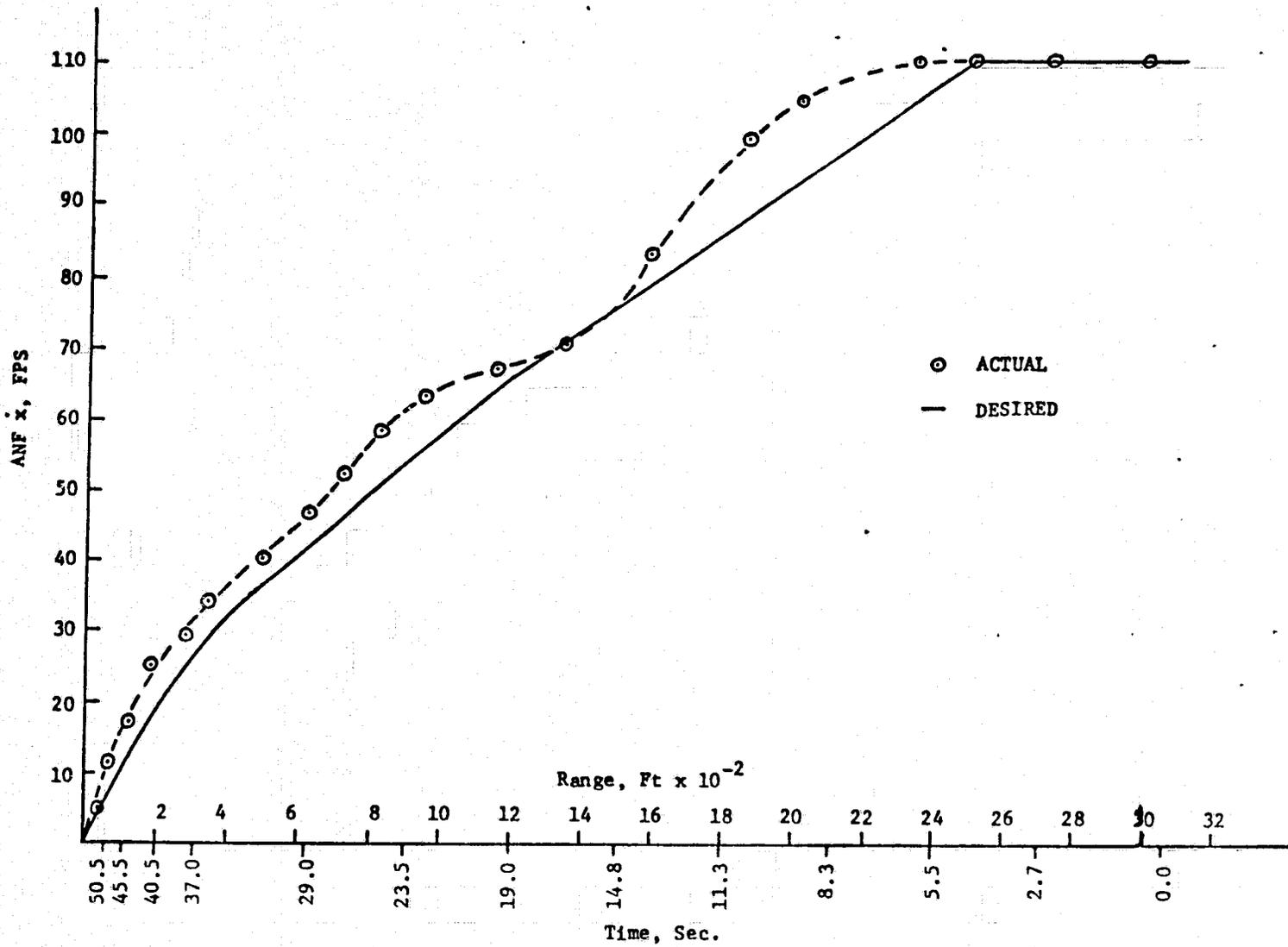
Figure (16) ANF Forward Velocity vs. Range
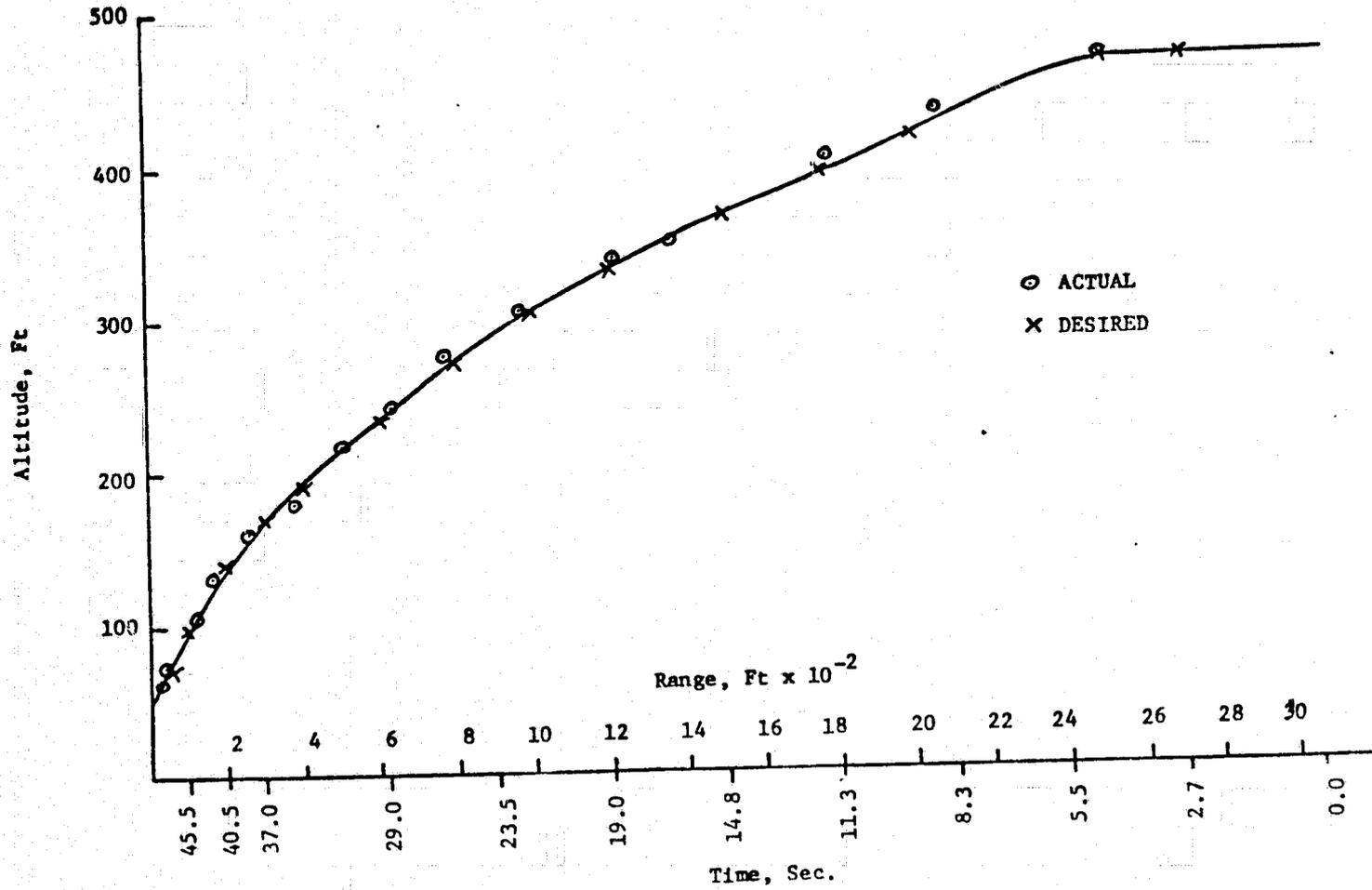
Figure (17) Altitude vs. Range
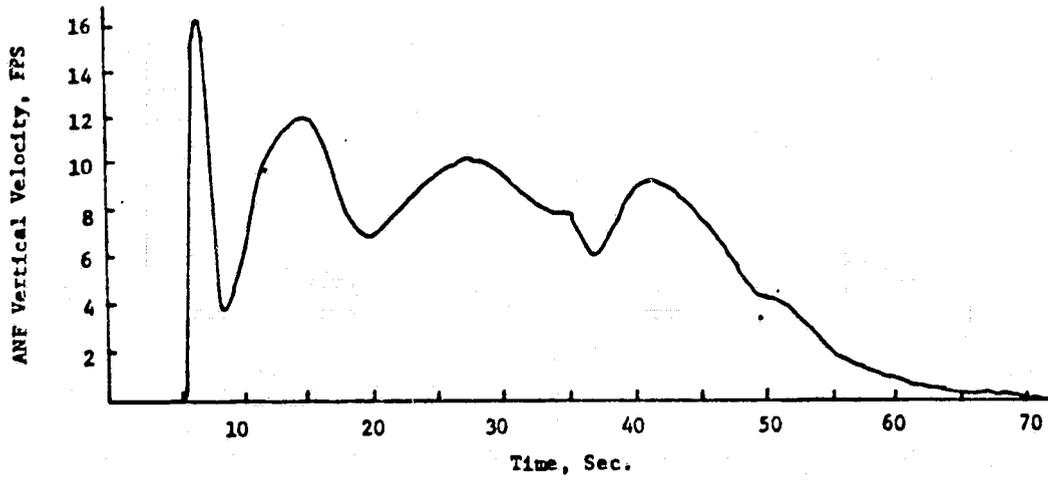
Figure (18) ANF ż vs. Time
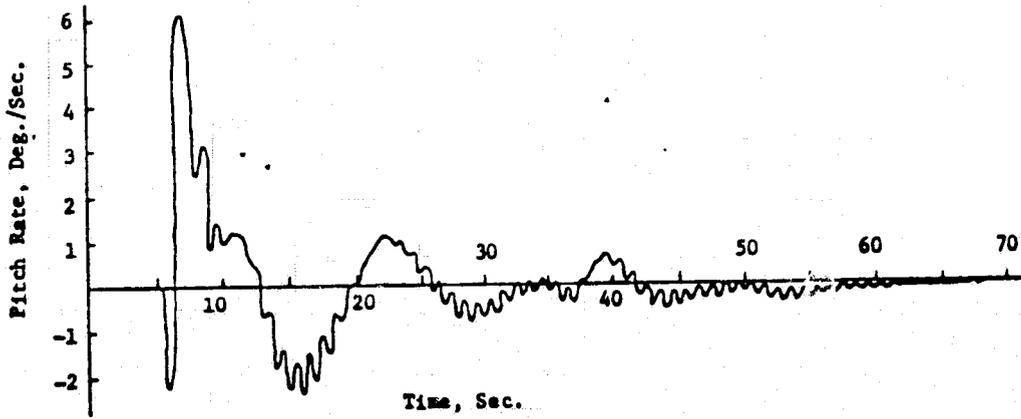
Figure (19) Pitch Rate vs. Time
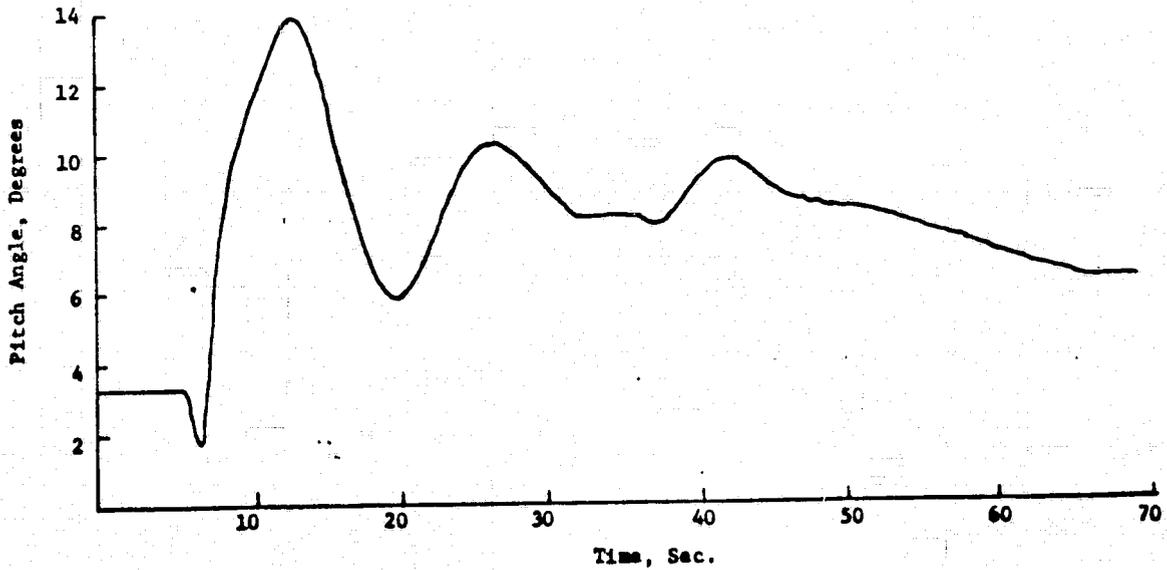
Figure (20) Pitch Angle vs. Time

35

feasibility of using the controller in an adaptive decelerating mode and it has demonstrated that this is possible. The remaining plots of ANF $\dot{z}$, pitch rate, and pitch angle vs. time are included to demonstrate that these values lie within acceptable limits.

Thus the controller appears capable of performing the functions it was designed for without exceeding the capabilities of the aircraft. The item remaining to be investigated is the controller's ability to function in the presence of errors in the estimates of aircraft parameters and at different sampling rates. The results of this study are presented in the next section.

6. SENSITIVITY STUDIES

Since the control algorithm is to be used in an on-board computer where the aircraft parameters must either be stored or estimated, it is necessary to have information concerning the controller's ability to function in the presence of errors in these parameters. The computer must also operate in real time and perform several functions in addition to the control function. Therefore it is necessary to know the controller's sensitivity to varying sampling rates. The results of these studies appear in this section.

6.1 Sensitivity to Parameter Errors

The linearized equations that describe the vehicle's motion about a nominal point are of the form of equation (2.1) which is written below in expanded form to show the actual entries in the A and G matrices.

$$
\begin{bmatrix} \dot{u} \\ \dot{w} \\ \dot{q} \\ \dot{\theta} \end{bmatrix}
=
\begin{bmatrix}
X_u/m & X_w/m & (X_{q}/m - W_n) & -g\cos\theta_n \\
Z_u/m & Z_w/m & (U_n + Z_{q}/m) & -g\sin\theta_n \\
M_u/I_{yy} & M_w/I_{yy} & M_q/I_{yy} & 0 \\
0 & 0 & 1 & 0
\end{bmatrix}
\begin{bmatrix} u \\ w \\ q \\ \theta \end{bmatrix}
+
\begin{bmatrix}
X_{\delta_e}/m & X_{\delta_c}/m \\
Z_{\delta_e}/m & Z_{\delta_c}/m \\
M_{\delta_e}/I_{yy} & M_{\delta_c}/I_{yy} \\
0 & 0
\end{bmatrix}
\begin{bmatrix} \delta_e \\ \delta_c \end{bmatrix}
$$

where

U_n = nominal forward velocity

W_n = nominal vertical velocity

θ_n = nominal pitch angle

g = gravitational acceleration

The remaining terms in the matrices are the stability and control derivatives that must be stored or estimated. The procedure used in the program was to specify U_n and W_n and use these values to determine θ_n and the derivatives based on the data in reference (12).

37

To determine the effect of errors in these parameters, values of U_n and W_n were specified and the necessary values of gain were calculated, using the techniques previously discussed. These gains, based on correct values of the vehicle's parameters, were then used to control the vehicle with the parameters changed, one by one, by multiplying by 0 and 3. This yields a fairly wide range of variation and should indicate the relative importance of each parameter.

The corresponding responses in forward and vertical velocity were plotted for velocity commands of $u_c = 10$ fps and $w_c = 0$ fps for nominal velocities of $U_n = 110$ fps and $W_n = 8.33$ fps. The sampling rate was 10 per second. These responses appear in figures (21) through (36) where each plot contains three curves representing the response with the correct value, the response with the indicated parameter set to zero and the response with the parameter multiplied by three.

Based on these curves it appears that the controller is fairly insensitive to variations in the vehicle parameters. For the stability derivatives, variations in the Z and M derivatives show considerable influence over the decoupling between u and w in steady state, but very little difference in the response for the first one or two seconds. If the controller is being flown in an adaptive mode, this may be the critical portion of the response since commands in u and w will most likely be updated every 0.5 to 1.0 seconds. The control derivatives Z_{δ_C}/m and M_{δ_E}/I_{yy} cause the vehicle to become unstable when set to zero. This however might have been expected since setting these parameters to zero severely limits the controller's ability to influence the vehicle's motion. The control derivative M_{δ_C}/I_{yy}, when multiplied by three, also caused the vehicle to become unstable. However, a factor of three error in a control derivative is

38
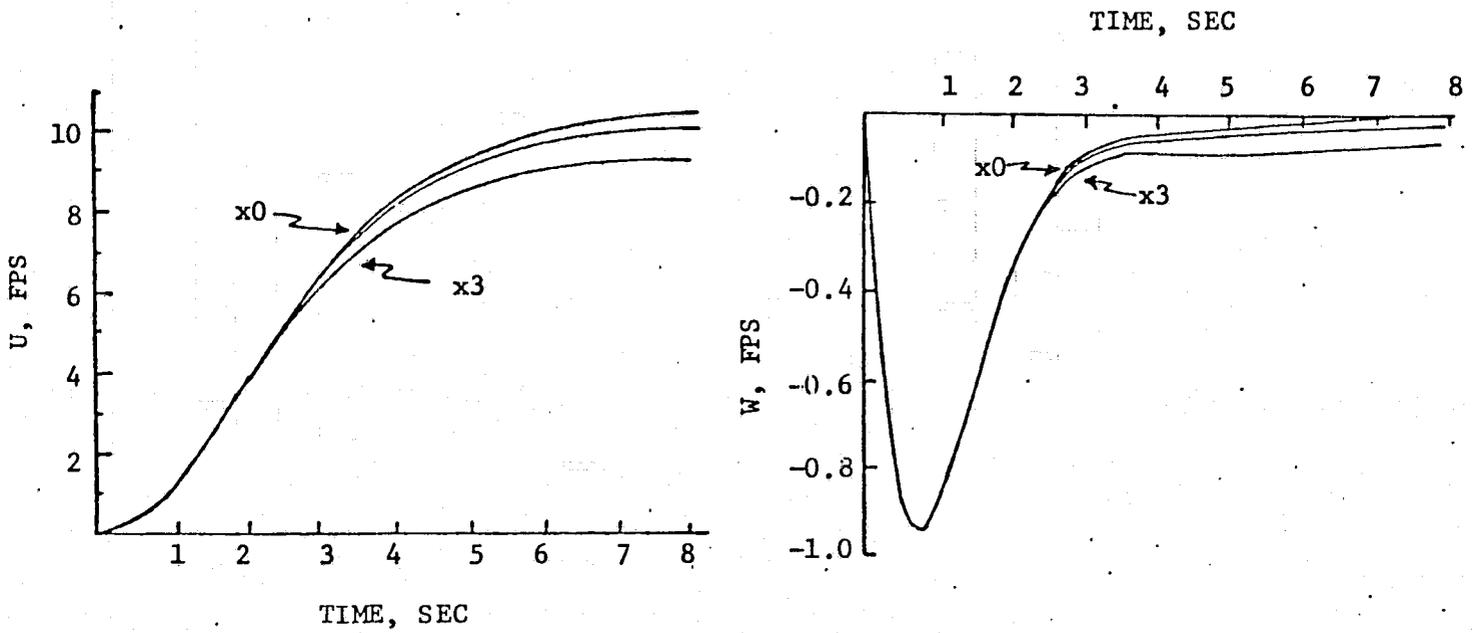
Figure (21) Velocity Responses to $\underline{u}_c^T = [10,0]$ With $X_{u/m}$ Changed
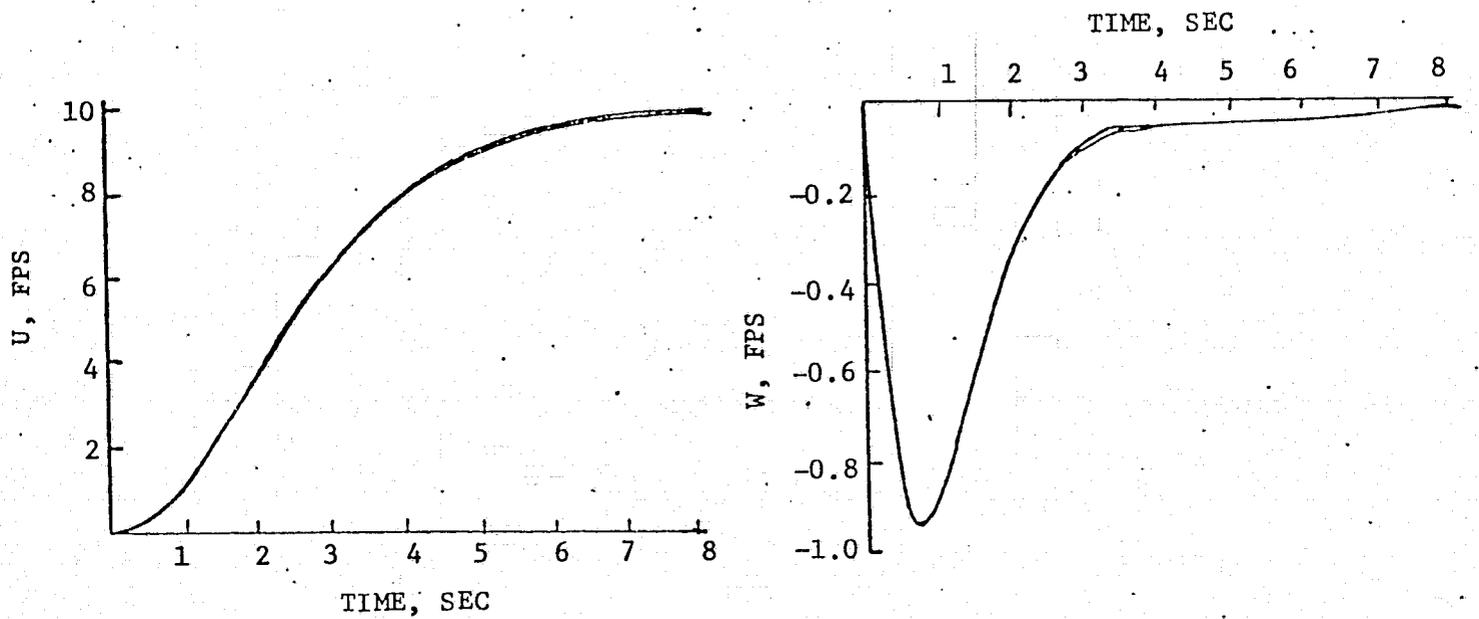
Figure (22) Velocity Responses to $\underline{u}_c^T = [10,0]$ With $X_{w/m}$ Changed
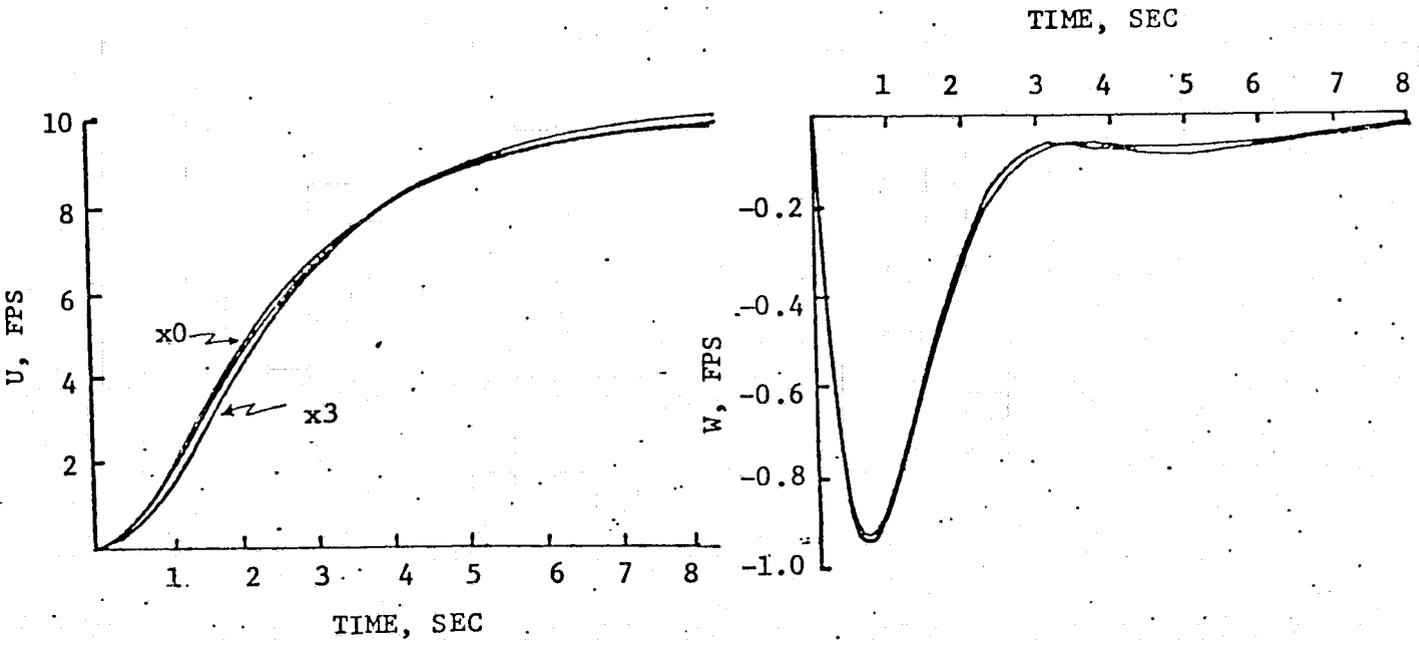
Figure (23) Velocity Responses to $\underline{u}_c^T = [10,0]$ With $X_{q/m}$ Changed
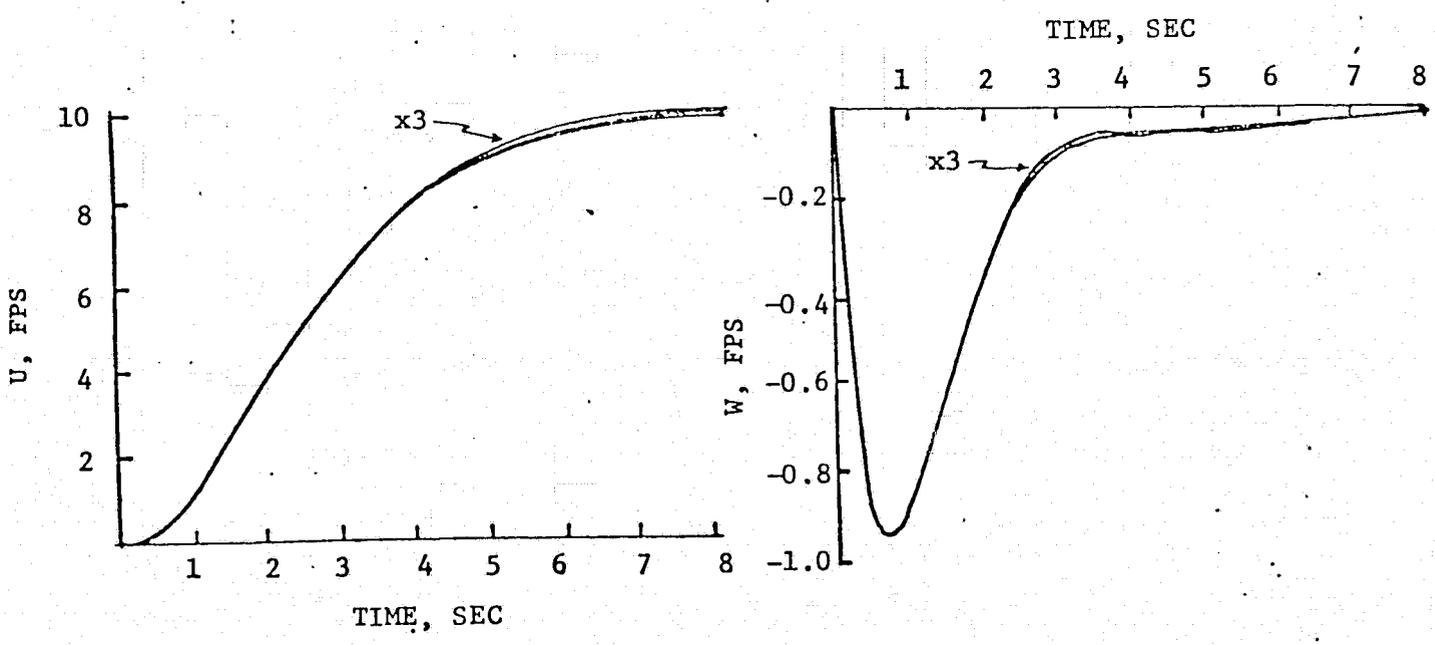
Figure (24) Velocity Responses to $\underline{u}_c^T = [10,0]$ With $X_{\delta_E/m}$ Changed
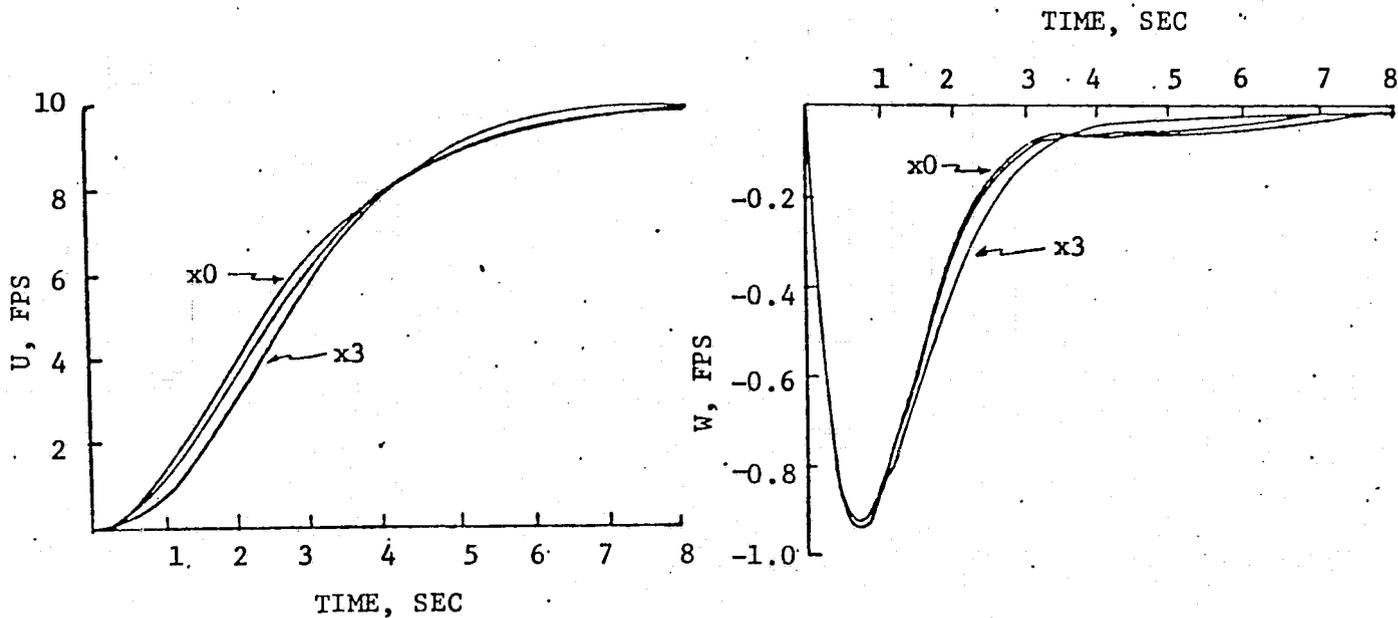
Figure (25) Velocity Responses to $\underline{u}_c^T = [10,0]$ With X_{δ_c}/m Changed
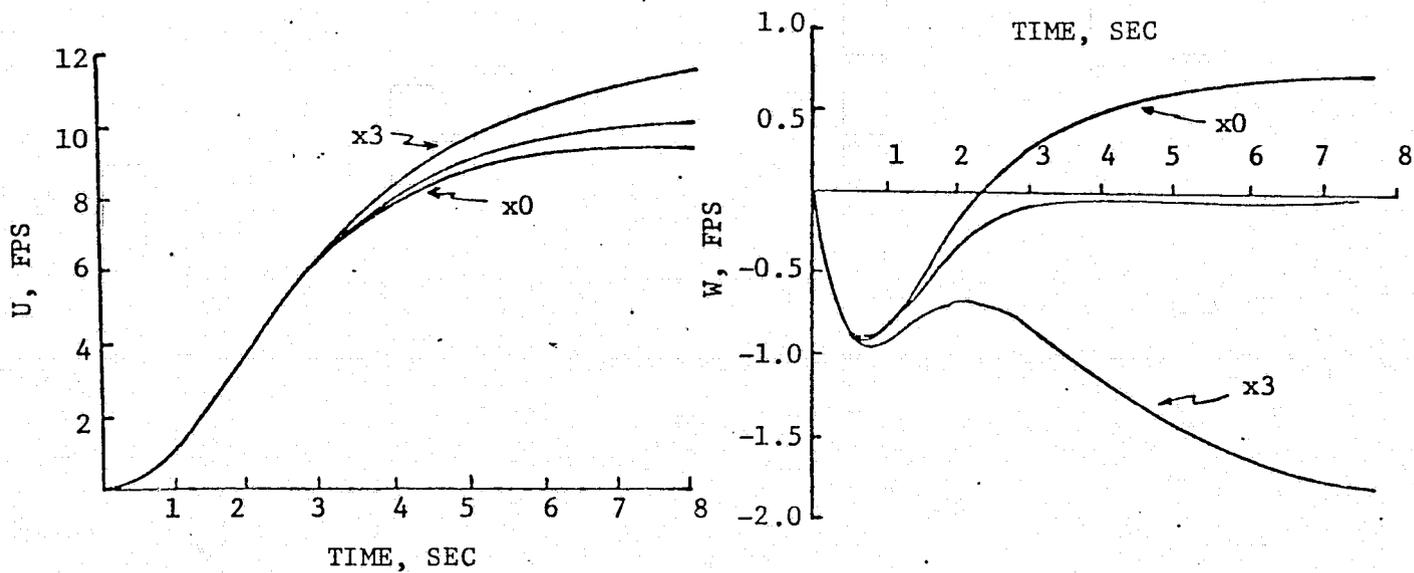
Figure (26) Velocity Responses to $\underline{u}_c^T = [10,0]$ With $Z_{u/m}$ Changed

41
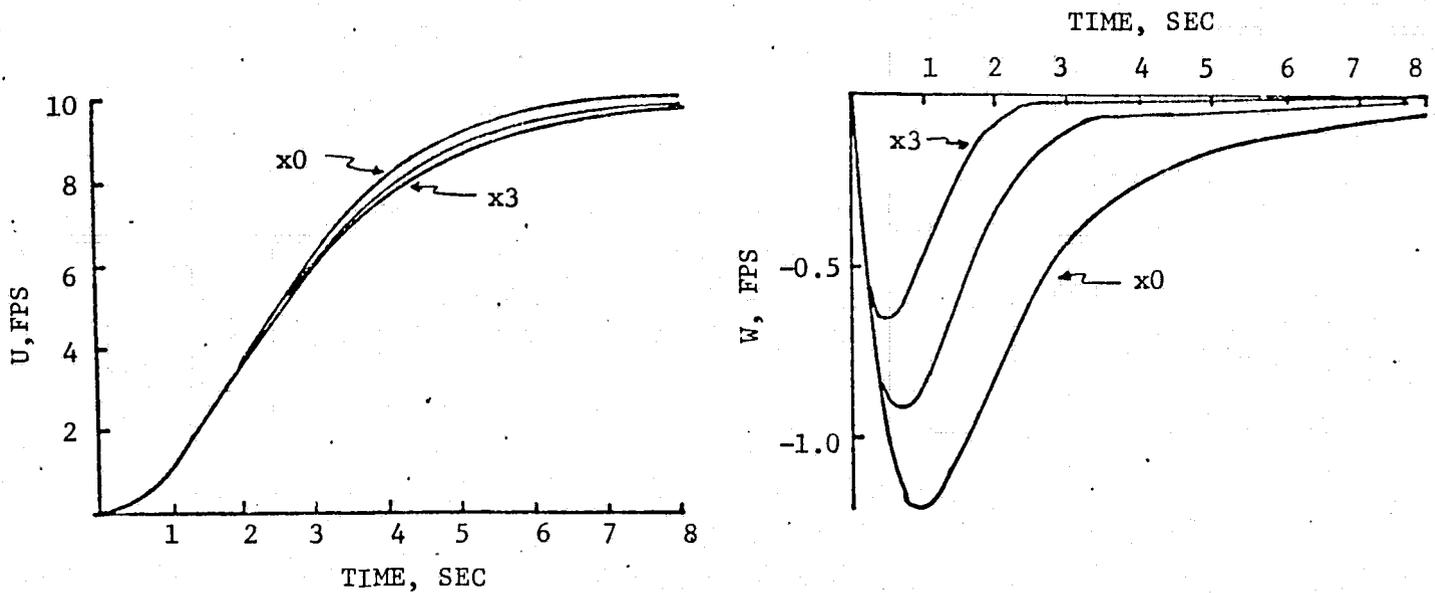
Figure (27) Velocity Responses to $\underline{u}_c^T = [10,0]$ With $Z_{w/m}$ Changed
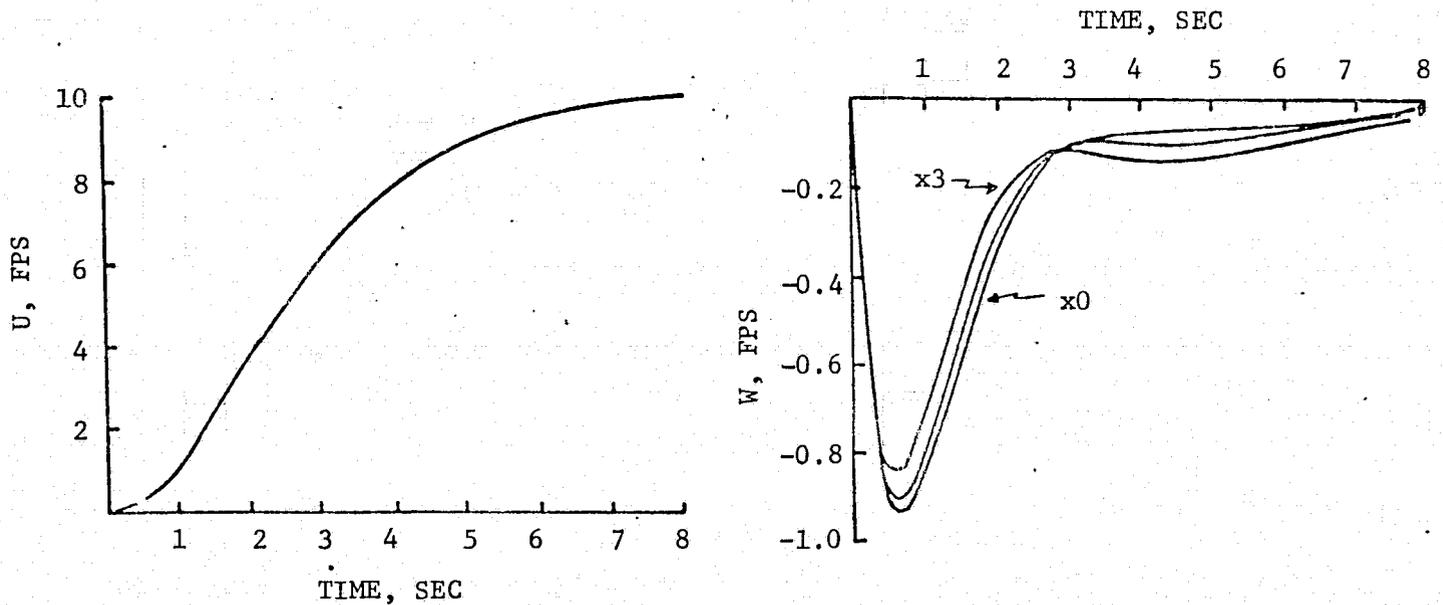
Figure (28) Velocity Responses to $\underline{u}_c^T = [10,0]$ With $Z_{q/m}$ Changed
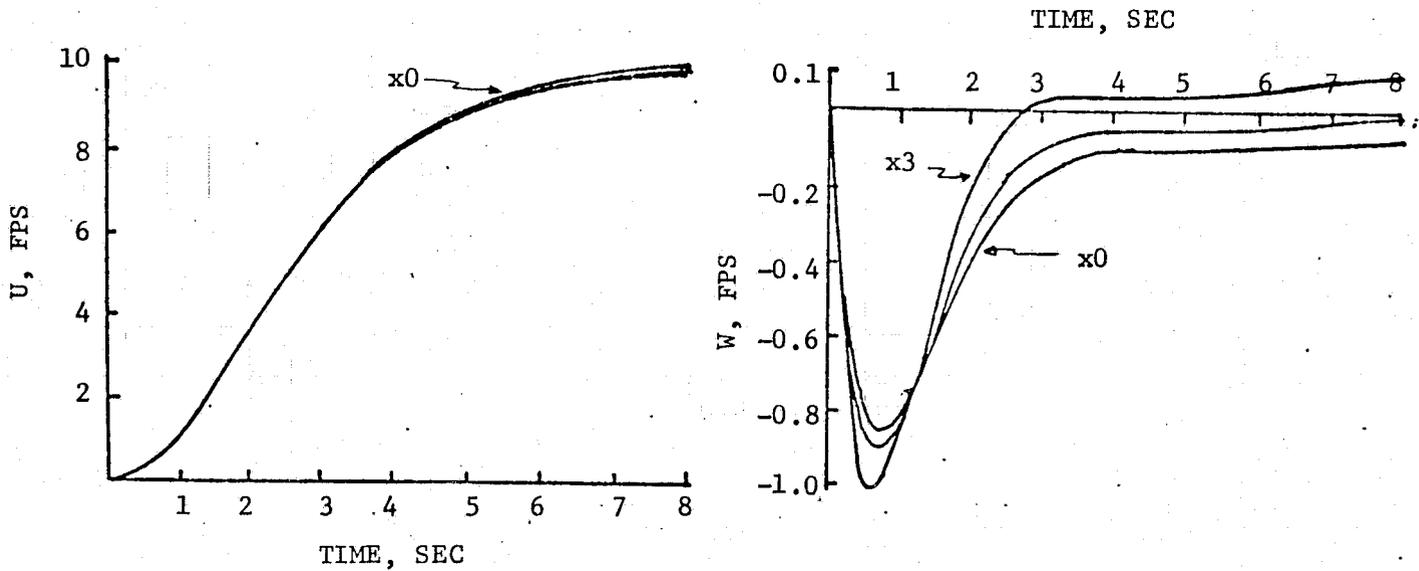
Figure (29) Velocity Responses to $\underline{u}_c{}^T = [10,0]$ With Z_{δ_E}/m Changed
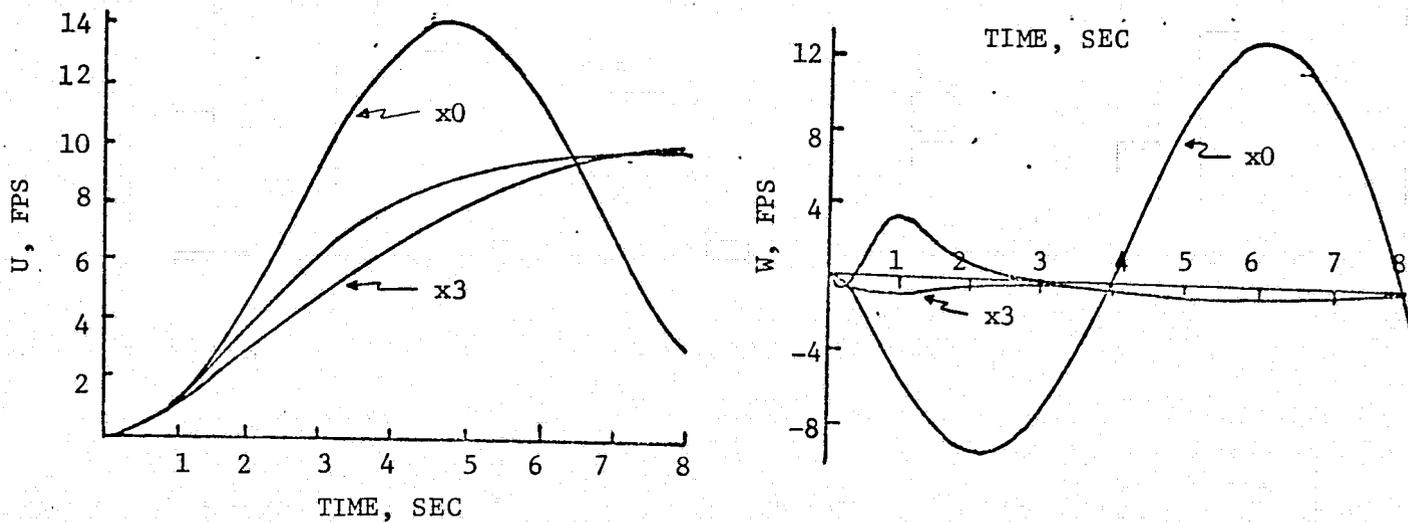
Figure (30) Velocity Responses to $\underline{u}_c{}^T = [10,0]$ With Z_{δ_c}/m Changed

43
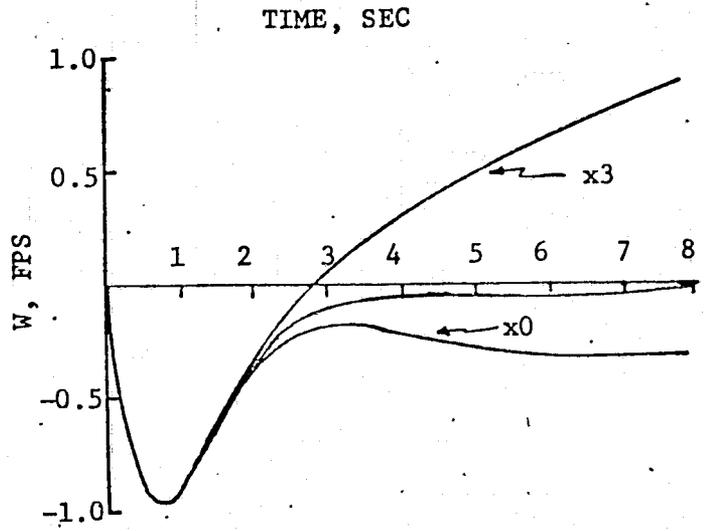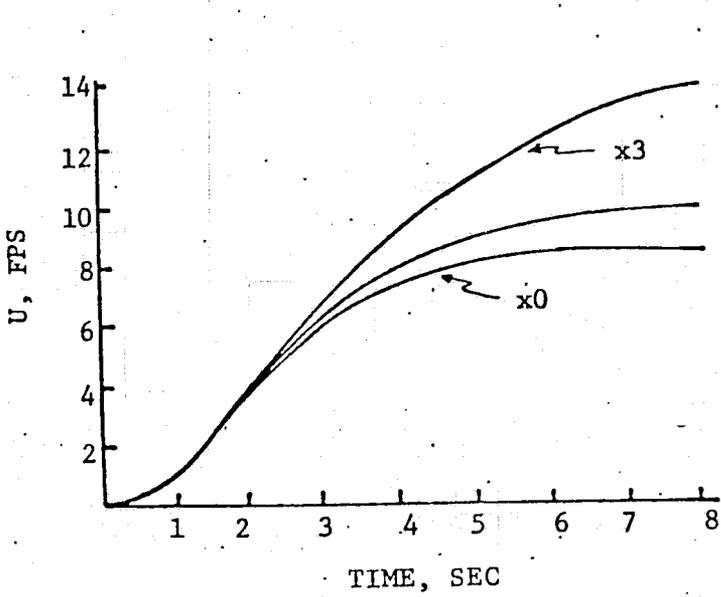
Figure (31) Velocity Responses to $\underline{u}_c{}^T = [10,0]$ With M_u/I_{yy} Changed
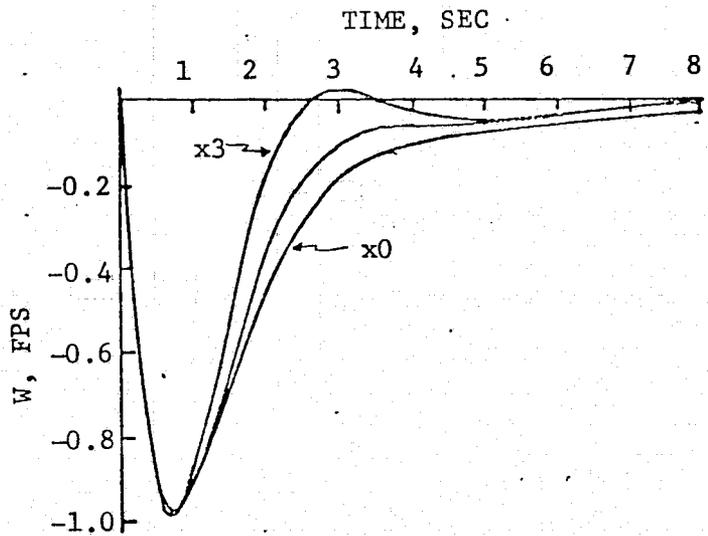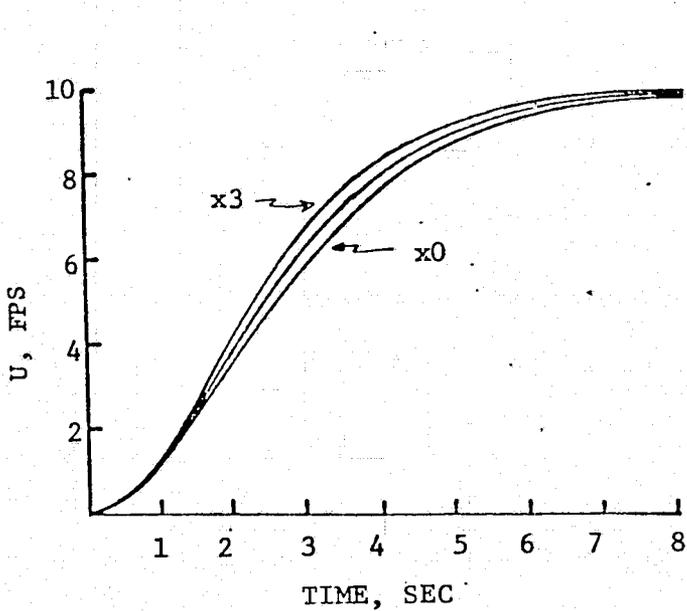
Figure (32) Velocity Responses to $\underline{u}_c{}^T = [10,0]$ With M_w/I_{yy} Changed

44
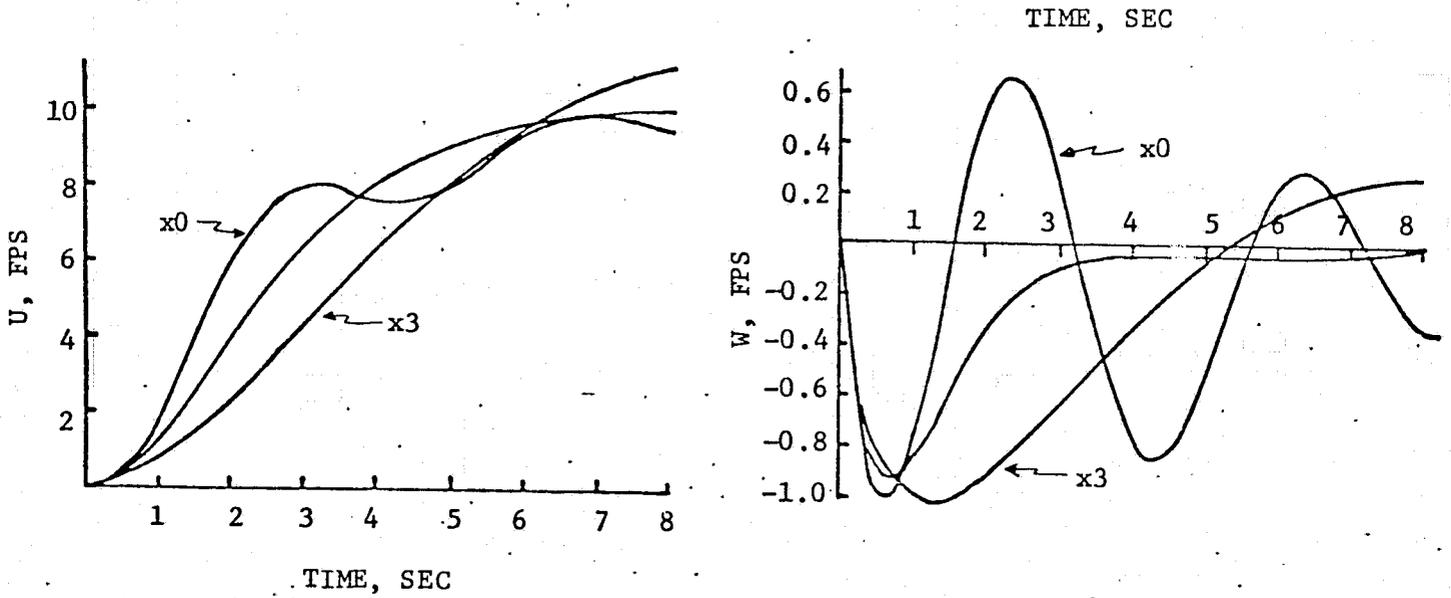
Figure (33) Velocity Responses to $\underline{u}_c{}^T = [10,0]$ With M_q/I_{yy} Changed
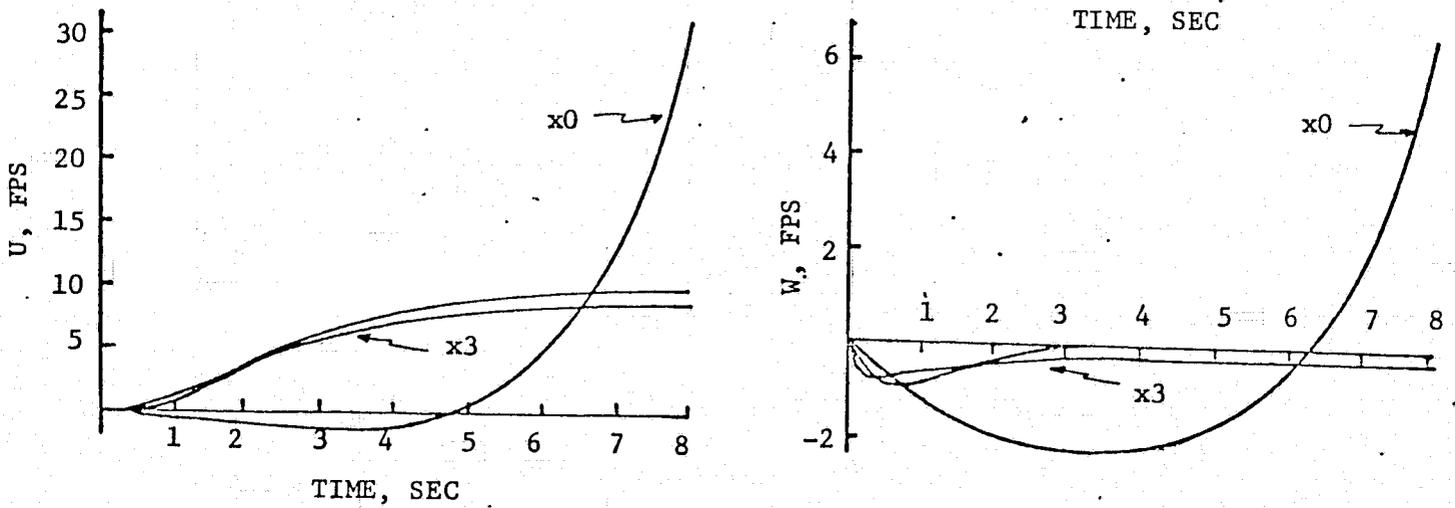
Figure (34) Velocity Responses to $\underline{u}_c{}^T = [10,0]$ With M_{δ_E}/I_{yy} Changed

45
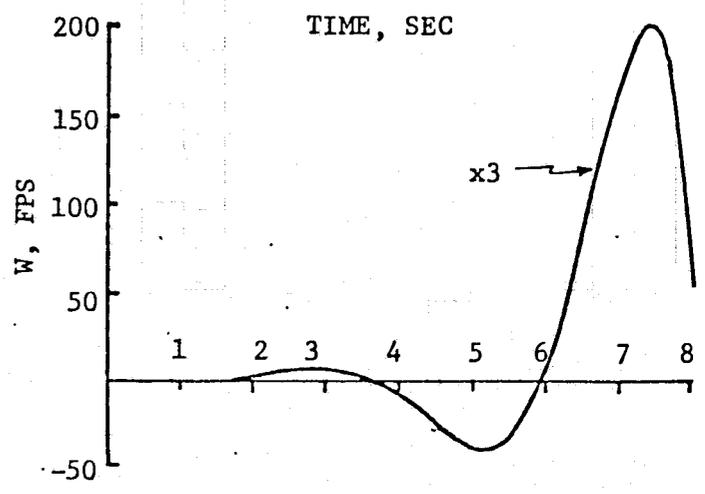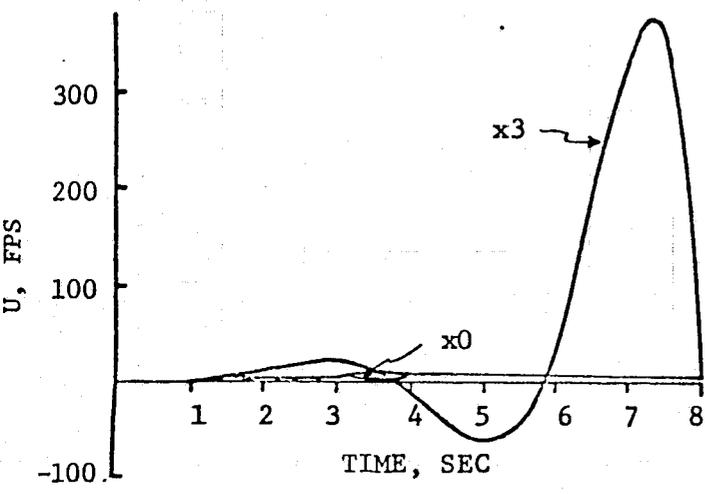
Figure (35) Velocity Responses to $\underline{u}_c^T = [10,0]$ With M_{δ_c}/I_{yy} Changed
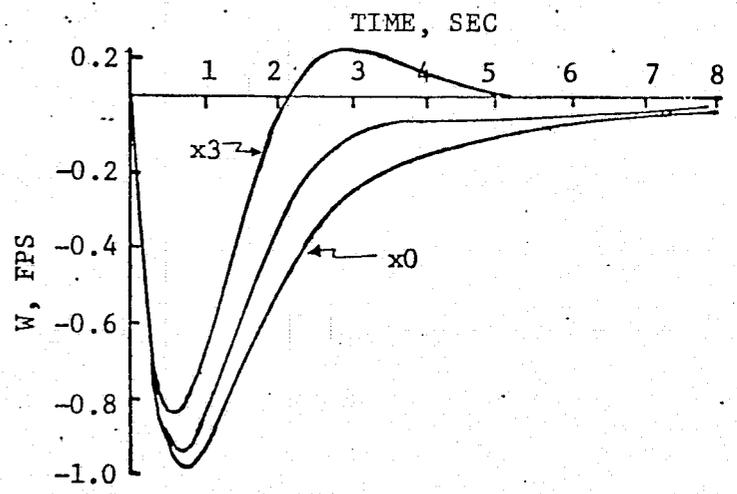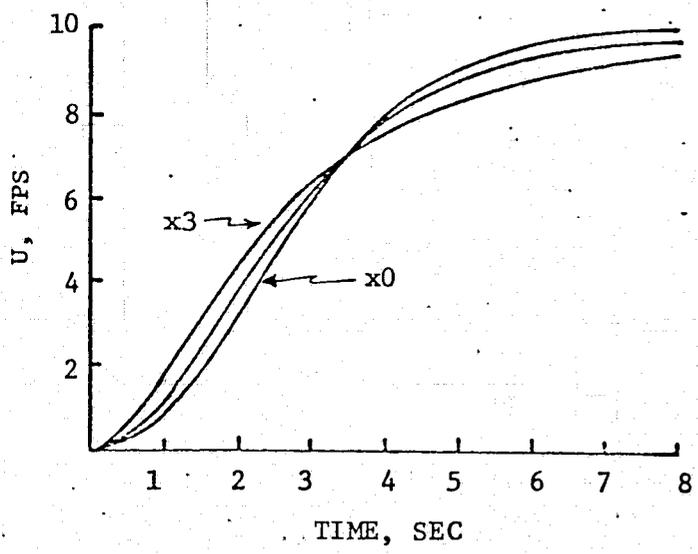
Figure (36) Velocity Responses to $\underline{u}_c^T = [10,0]$ With θ_n Changed

an extreme variation.

The above results are admittedly limited in their application since the vehicle parameters were varied one by one. They should however serve to indicate the relative importance of the parameters. It is recommended that work in this area be continued.

6.2 Sensitivity to Sampling Rate

Using the procedures described in this report the gains are calculated assuming a continuous system with dynamics described by equation 2.1, rewritten below.

$$\dot{x} = A\underline{x} + G\underline{\delta} \tag{2.1}$$

Since the actual system, however, is digital, the equations of motion become

$$\underline{x}_{i+1} = F \, \underline{x}_i + B \, \underline{\delta}_i \tag{6.1}$$

where

$$F = \int_0^T AF \, dt \qquad F_o = I \tag{6.2}$$

$$B = \int_0^T (AB + G) \, dt \quad B_o = 0 \tag{6.3}$$

with T being the sample time. Thus the procedure was to calculate the gains for a continuous system and use those gains to generate $\underline{\delta}_i$ in equation (6.1) using the following equation

$$\underline{\delta}_{i+1} + 1 = K \, \underline{x}_i + K_2 \, \underline{\delta}_{ci} \tag{6.4}$$

Equation (6.4) can represent the input for the velocity command controller by setting K_2 equal to the feedforward gain matrix and letting $\underline{\delta}_{ci}$ be a vector of velocity commands or it can represent the input for pilot commands by setting K_2 equal to an identity matrix and letting $\underline{\delta}_{ci}$ be the vector of pilot inputs.

Applying the input of equation (6.4) to equation (6.1) the state responses were plotted for different sampling rates by generating new F and B matrices using equations (6.2) and (6.3). Responses were plotted for values of T between 0.05 and 2.0 sec at nominal velocities of U_n = 20 fps, W_n = 3.33 fps and U_n = 110 fps, W_n = 8.33 fps.

For nominal velocities of U_n = 20 fps and W_n = 3.33 fps there is very little change in the vehicle's response for values of T of 0.5 second and smaller. The responses for T = 1.0 second were still stable but were becoming oscillatory and at T = 2.0 seconds the system was unstable. At the higher velocities of U_n = 110 fps and W_n = 8.33 fps the responses had become oscillatory at T = 0.5 second and unstable at T = 1.0 second. For T = 0.33 second and below, however, there was little difference indicating that these rates should be acceptable at all points along the approach trajectory.

7. CONCLUSIONS

A technique has been developed for generating feedback and feedforward gains capable of producing acceptable vehicle responses to both pilot and guidance system commands. The calculations are simple and lend themselves to on-board computation in an adaptive mode of operation. Sensitivity studies indicate that the system can function in the presence of errors in vehicle parameters and over a fairly wide range of sampling intervals.

Publications

The results of this work have been published as listed below in reference 8 and in the paper "A Velocity Command Controller For A VTOL Aircraft" presented at the 1976 JACC, West Lafayette, Indiana, July 1976.

Technical Officer

The NASA technical officer for this grant was Dr. J. F. Creedon, M.S. 494, NASA Langley Research Center, Hampton, Virginia.

REFERENCES

1. Anon., "Northeast Corridor VTOL Investigation," Civil Aeronautics Board, February 2, 1970.

2. Marsh, K.R., "Study on the Feasibility of V/STOL Concepts for Short-Haul Transport Aircraft," NASA CR-670, January, 1967.

3. Montgomery, R.C., "Introduction to Linear System Analysis and Design By Use of State Vector Approach," Chapter 10 of NASA SP-258, Performance and Dynamics of Aerospace Vehicles, 1971.

4. Montgomery, R.C., and Hatch, H.G., Jr., "The Application of a Differential Synthesis Technique to the Design of Multiaxis Stability Augmentation Systems," Journal of Aircraft; Vol. 6, No. 4, 1969, pp. 336-342.

5. Chen, R.T.N., "A Method of Pole-Zero Placement For Multivariable Control Systems," Proc. 1971 JACC, pp. 901-907, August, 1971.

6. Reid, G.F., "Digital Adaptive Control of a VTOL Aircraft," Semiannual Progress Report for the period November 1973-April 1974 for NASA Grant NGR 47-018-005, May, 1974.

7. Reid, G.F., "Digital Adaptive Control of a VTOL Aircraft," Semiannual Progress Report for the period May-November 1974 for NASA Grant NGR 47-018-005, December, 1974.

8. Reid, G.F., "A Technique For Pole-Zero Placement For Dual-Input Control Systems," presented at SOUTHEASCON 76, April 1976.

9. Kelly, J.R., Niessen, F.R., and Garren, J.F., Jr., "A Manual-Control Approach to Development of VTOL Automatic Landing Technology," presented at the 29th Annual National Forum of The American Helicopter Society, Washington, D.C., May, 1973.

10. Anon., "V/STOL Handling, I-Criteria and Discussion," AGARD-R-577-70.

11. Reid, G.F., "Digital Adaptive Control of a VTOL Aircraft," Semiannual
     Progress Report for the period December 1974-May 1975 for NASA Grant
     NGR 47-018-005, May, 1975.

12. Ostroff, A.J., Downing, D.R., and Rood, W.J., "A Technique Using A
     Nonlinear Helicopter Model For Determining Trims and Derivatives,"
     NASA TN D-8159, May, 1976.

13. Hoffman, W.C., Zvara, J., Bryson, A.E., Jr., and Ham, N.D., "Automatic
     Guidance Concept for VTOL Aircraft," Journal of Aircraft, Vol. 8, No. 8,
     August, 1971, pp. 637-642.

A TECHNIQUE FOR POLE-ZERO PLACEMENT

FOR DUAL-INPUT CONTROL SYSTEMS

Gerald F. Reid

Virginia Military Institute

Lexington, Virginia

ABSTRACT

An algorithm is presented for determining the feedback gains required to place the poles and zeros, of pre-selected transfer functions of a dual-input control system, at arbitrary locations in the S-plane. The technique employs Leverrier's algorithm and has been used in a digital simulation to control the longitudinal dynamics of the CH-47 helicopter.

A VELOCITY-COMMAND CONTROLLER FOR A VTOL AIRCRAFT

Gerald F. Reid

Virginia Military Institute

Lexington, Virginia

ABSTRACT

A technique is presented for calculating feedback and feedforward gain
matrices that enable a VTOL aircraft to track input commands of forward and
vertical velocity while maintaining acceptable responses to pilot inputs.
Leverrier's algorithm is used for determining a set of state-variable, feed-
back gains that force the closed-loop poles and zeros of one pilot-input
transfer function to pre-selected positions in the s-plane. This set of
feedback gains is then used to calculate the feedback and feedforward gains
for the velocity-command controller. The method is computationally attractive
since the gains are determined by solving systems of linear, simultaneous
equations. The method has been used in a digital simulation of the CH-47
helicopter to control longitudinal dynamics.